Cerebral Cortex August 2011;21:1840–1856
doi:10.1093/cercor/bhq254
Advance Access publication January 18, 2011

The Cyclin-Dependent Kinase Inhibitor p57^{Kip2} Regulates Cell Cycle Exit, Differentiation, and Migration of Embryonic Cerebral Cortical Precursors

Anna Tury, Georges Mairet-Coello and Emanuel DiCicco-Bloom

Department of Neuroscience and Cell Biology, University of Medicine and Dentistry of New Jersey-Robert Wood Johnson Medical School, Piscataway, NJ 08854, USA

Address correspondence to Anna Tury, Department of Neuroscience and Cell Biology, University of Medicine and Dentistry of New Jersey-Robert Wood Johnson Medical School, Piscataway, NJ 08854, USA. Email: turyanna@hotmail.com.

Mounting evidence indicates cyclin-dependent kinase (CDK) inhibitors (CKIs) of the Cip/Kip family, including p57^{Kip2} and p27^{Kip1}, control not only cell cycle exit but also corticogenesis. Nevertheless, distinct activities of p57^{Kip2} remain poorly defined. Using in vivo and culture approaches, we show p57^{Kip2} overexpression at E14.5–15.5 elicits precursor cell cycle exit, promotes transition from proliferation to neuronal differentiation, and enhances process outgrowth, while opposite effects occur in p57^{Kip2}-deficient precursors. Studies at later ages indicate p57^{Kip2} overexpression also induces precocious glial differentiation, suggesting stage-dependent effects. In embryonic cortex, p57^{Kip2} overexpression advances cell radial migration and alters postnatal laminar positioning. While both CKIs induce differentiation, p57^{Kip2} was twice as effective as p27^{Kip1} in inducing neuronal differentiation and was not permissive to astrogliogenic effects of ciliary neurotrophic factor, suggesting that the CKIs differentially modulate cell fate decisions. At molecular levels, although highly conserved N-terminal regions of both CKIs elicit cycle withdrawal and differentiation, the C-terminal region of p57^{Kip2} alone inhibits in vivo migration. Furthermore, p57^{Kip2} effects on neurogenesis and gliogenesis require the N-terminal cyclin/CDK binding/inhibitory domains, while previous p27^{Kip1} studies report cell cycle-independent functions. These observations suggest p57^{Kip2} coordinates multiple stages of corticogenesis and exhibits distinct and common activities compared with related family member p27^{Kip1}.

Keywords: gliogenesis, in utero electroporation, neurite outgrowth, neurogenesis, transfection

Introduction

During development of the rat cerebral cortex, neurons and glia are generated sequentially, with neurogenesis occurring primarily in the embryo and gliogenesis postnatally. Projection neurons of the 6 cortical layers are generated from dividing progenitors of the underlying ventricular (VZ) and subventricular zones (SVZ) in an inside-out fashion (Angevine and Sidman 1961; Rakic 1974). Since cell type and laminar fate depend on the time of terminal division (McConnell and Kaznowski 1991), signals regulating cell cycle withdrawal may also impart cell fate determination (Ohnuma et al. 2001).

Cell cycle progression is driven by cyclin/cyclin-dependent kinase (CDK) complexes whose activities are negatively regulated through associations with CDK inhibitors (CKIs). CKIs of the Cip/Kip family, including p21^{Cip1} (p21), p27^{Kip1} (p27), and p57^{Kip2} (p57), block activities of multiple cyclin/CDK complexes (Sherr and Roberts 1999). By binding cyclin E/CDK2 complexes, Cip/Kip proteins prevent G1/S-phase transition and induce cell cycle withdrawal. While family members share a conserved N-terminal domain that binds and inhibits cyclin/CDK complexes, they diverge in C-terminal regions, suggesting distinct functions and mechanisms (Besson et al. 2008). Moreover, 3 alternative splice isoforms of p57 transcript have been uncovered in the rat that generate N-terminal heterogeneity (Potikha et al. 2005), but their functions remain undefined. The roles of Cip/Kip proteins in controlling cell proliferation are well documented (Nakayama et al. 1996; Sherr and Roberts 1999). In addition, CKIs regulate cell differentiation, migration, and apoptosis in several peripheral tissues (Zhang et al. 1997; Besson et al. 2008) and play similar roles during brain development. Cip/Kip proteins regulate gliogenesis, including cortical astrocyte proliferation (Koguchi et al. 2002), cortical oligodendrocyte differentiation (Casaccia-Bonnefil et al. 1997; Zezula et al. 2001; Dugas et al. 2007) and retinal Müller glial cell determination (Ohnuma et al. 1999). Several studies also highlight the importance of Cip/Kip proteins in neurogenesis. p27 regulates neuronal differentiation and radial migration in mouse neocortex, involving 2 distinct domains and mechanisms (Nguyen et al. 2006). In the retina, p57 regulates development of a restricted subset of amacrine interneurons (Dyer and Cepko 2000, 2001). In the midbrain, p57 influences differentiation and survival of dopamine neurons by cooperating with orphan nuclear receptor Nurr1 (Joseph et al. 2003), while in cortical precursors, it may mediate cell cycle exit elicited by antimitogenic signals (Carey et al. 2002). While gene knock down experiments suggested the involvement of p57 in cortical migration (Itoh et al. 2007), a role in cortical differentiation remains undefined.

In this study, using overexpression approaches and p57-deficient cortical cells, we report that p57 participates in multiple events of corticogenesis. In addition to eliciting cell cycle exit, p57 induced precocious cell differentiation, process outgrowth, and radial migration of rodent cortical progenitors. Comparison with related family member p27 indicates that the 2 CKIs have both overlapping as well as nonredundant activities during corticogenesis. While both induced neuronal and glial differentiation, p57 promoted more neuronal differentiation than p27. Moreover, p57 blocked the astrogliogenic effects of ciliary neurotrophic factor (CNTF) contrary to p27, suggesting that the 2 CKIs modulate cell fate decisions differentially in a context-dependent manner. Finally, in contrast to p27 (Nguyen et al. 2006), the differentiation and migration functions of p57 both require the cyclin/CDK binding/inhibitory domains.

Materials and Methods

Animals

Time-mated pregnant Sprague Dawley rats were obtained from Hilltop Lab Animals. p57-deficient mice were obtained from Zhang et al.

(1997). p57 is a maternally expressed imprinted gene so that heterozygous mutants with a defective maternal allele (p57+/m–) exhibit the same phenotype as homozygous p57–/– mutants (Zhang et al. 1997). Studies were performed on wild type (WT) and p57+/m– (p57KO) heterozygous littermates obtained by crossing WT males with p57+/p– females. Genotypes were determined by standard polymerase chain reaction (PCR), as described previously (Zhang et al. 1997). p27+/– mice were obtained from The Jackson Laboratory (reference number: 003122) and genotyped as previously described (Fero et al. 1996). Specificity of p27 antibodies was verified on p27 homozygous null mutant brains (p27KO).

The day of vaginal plug detection was considered E0.5. Animals were housed in a temperature-controlled room with standard laboratory food and water provided ad libitum. All animal manipulations and experimental procedures were performed in accordance with the guidelines for animal experimentation of IACUC and NIH.

Plasmid Constructs

cDNAs corresponding to coding regions of p27 (NCBI accession number NM_004064, 597 bp from 466 bp to 1062 bp), p57 (U20553, 1047 bp from 41 bp to 1087 bp), and Ngn2 (NM_009718, 792 bp from 315 bp to 1106 bp) were inserted into pCIG2 plasmid (Hand et al. 2005) between *XhoI* and *EcoRI* restriction sites. pCIG2 vector, which was modified from pCIG vector (Megason and McMahon 2002), contains an internal ribosomal entry site and the enhanced green fluorescence protein (EGFP) under the control of a chicken β-actin promoter and an cytomegalovirus-immediate early enhancer. We also subcloned in pCIG2 plasmid between the same restriction sites the N-terminal region of p57 cDNA (Nterp57) which corresponds to the cyclin/CDK inhibitory domain (U20553, 342 bp from 41 bp to 382 bp) and its C-terminal region (Cterp57), corresponding to p57 devoid of the cyclin/CDK inhibitory domain (U20553, 792 bp from 296 bp to 1087 bp). In addition, we generated a p57 mutant vector (p57CK-) deficient for interaction with both cyclins (R33A and F36D, NCBI accession number AAC52186) and CDKs (W63A and F67D), by site-directed mutagenesis as described previously (Watanabe et al. 1998; Nguyen et al. 2006). Sequences and point mutations were verified by DNA sequencing (GENEWIZ). Plasmids were extracted and purified using EndoFree plasmid Maxi kit (Qiagen).

Cortical Cell Culture

At E14.5 or E17.5, rat or mouse pregnant females were sacrificed by CO_2 asphyxia and embryos were removed from uterine horns. Skin, skull, and meninges were removed from embryo heads. The dorsolateral cortex was dissected and mechanically dissociated using a fire-polished glass pipette. Before dissociation, E17.5 cortices were digested with trypsin (0.25 mg/mL, Worthington) for 20 min followed by trypsin inhibitor (1 mg/mL, Sigma) incubation for 2 min.

For quantitative reverse transcriptase-polymerase chain reaction (Q-RT-PCR) analysis, rat cortical cells were plated at 1750 cells/mm^2 (1.7 millions cells/dish) on poly-D-lysine (100 μg/mL, Sigma)-coated 35 mm dishes, in defined medium, as previously described (Lu and DiCicco-Bloom 1997; Mairet-Coello et al. 2009). Culture medium was composed of a 50:50 (v/v) mixture of DMEM and F12 (Invitrogen) containing penicillin (50 U/mL, Invitrogen) and streptomycin (50 μg/mL, Invitrogen) and supplemented with transferrin (100 μg/mL, Calbiochem), putrescine (100 μM, Sigma), progesterone (20 nM, Sigma), selenium (30 nM, Sigma), glutamine (2 mM, Invitrogen), glucose (6 mg/mL, Sigma), and bovine serum albumin (10 mg/mL, Sigma). Cultures were maintained in a humidified 5% CO_2/air incubator at 37 °C. Cells were incubated for 24 h with basic fibroblastic growth factor (bFGF, 10 ng/mL, Scios), pituitary adenylate cyclase-activating polypeptide (PACAP, 10^{-8} M, American Peptide), or neurotrophin-3 (NT3, 10 ng/mL, PeproTech). To study the effect of mitogen withdrawal on CKI expression, cells were incubated in presence of bFGF (10 ng/mL) for 24 h, rinsed twice with medium without bFGF and incubated in absence of bFGF for 24 h. Control cultures were rinsed and replaced with medium containing bFGF, at the same time.

For neurite outgrowth studies of p57-deficient cells, individual cortices were dissected, dissociated, and plated separately from mouse embryos whose genotype was determined after the experiment. Cells were plated at a density of 104 cells/mm^2 (100 000 cells/dish) on poly-D-lysine (5 μg/mL)-coated 35 mm dishes and incubated for 24 h in defined medium as described above. Then, cells were fixed with ice-cold 4% paraformaldehyde (PFA, Sigma) prepared in 0.1 M phosphate buffered saline (PBS) for 20 min and washed with PBS. For studies of differentiation and process length of nestin+ and TuJ1+ cells, WT and p57-deficient cells were grown on poly-D-lysine-coated 35 mm dishes in Neurobasal/B27 (Invitrogen) medium containing bFGF as described below and fixed at 48 h.

In Vitro Transfection

E14.5 or E17.5 rat cortical cells were plated at a density of 815 cells/mm^2 (400 000 cells/coverslip) on poly-D-lysine (100 μg/mL) and laminin (16 μg/mL, Invitrogen)-coated 25 mm glass coverslips and incubated in Neurobasal/B27 medium containing bovine serum albumin (1 mg/mL), glutamine (2 mM), penicillin (25 U/mL), streptomycin (25 μg/mL), and bFGF (10 ng/mL). Two hours after plating, cells were washed with Neurobasal/glutamine medium and transfected in Neurobasal/glutamine/B27 containing Lipofectamine LTX and Plus Reagents (Invitrogen) with pCIG2 plasmids (1 μg/mL). Five hours later, reaction medium was replaced with plating medium, and cells were incubated for 24 h or 48 h. To assess S-phase entry, some coverslips were incubated with 10 μM Bromodeoxyuridine (BrdU, Sigma) for the last 4 h of cultures. To study the effects of CKIs on glial differentiation, CNTF (10 ng/mL, Calbiochem) was added after transfection to the growth media (containing bFGF) to promote astrocyte differentiation (Bonni et al. 1997; Song and Ghosh 2004). Cells were fixed with ice-cold 4% PFA for 20 min and washed in PBS.

In Utero Electroporation

Pregnant rats at E15.5 or E18.5 were anaesthetized with a mix of ketamine (100 mg/kgbw, Ketaset, Fort Dodge Animal Health) and xylasine (10 mg/kgbw, Xyla-Ject, Phoenix Pharmaceuticals). Uterine horns were exposed by laparotomy, and embryos were transilluminated to visualize the cerebral cortex. Three microliters of plasmid solution (diluted at 1 μg/μl in 0.1 M PBS pH 7.2, containing 0.05% fast green dye, MP Biochemicals) were manually microinjected into the right or the left lateral ventricle (LV) through the uterine wall, using a Hamilton syringe (33/1′′/PT4). Injections were considered successful when the dye spread into the contralateral ventricle. Immediately after injection, 5 electric pulses (50 V, 50 ms) were delivered at a rate of one pulse per second by a square wave electroporation system ECM 830 (BTX, Harvard Apparatus). After electroporation, the uterine horns were returned to the abdominal cavity, and muscle and skin were sutured. To minimize pain and discomfort, animals were given Rimadyl (2 mg/tablet). At the indicated times (1–4 days after electroporation), pregnant females were sacrificed by CO_2 asphyxia and embryos were removed. Brains were dissected, fixed by immersion in 4% PFA-PBS overnight at 4 °C, and transferred to a 30% sucrose-PBS cryoprotective solution for 1 day at 4 °C. For postnatal analyses, postnatal day 10 (P10) pups were anaesthetized with a mix of ketamine/xylasine and perfused through the left ventricle with 0.9% NaCl followed by 4% PFA-PBS. Brains were postfixed in the same fixative for 1 h and immersed in 30% sucrose-PBS overnight at 4 °C. Embryonic and P10 brains were embedded in optimal cutting temperature compound (Tissue Tek, Sakura Finetek) and frozen on dry ice. Brains were cut into 12-μm coronal sections with a cryostat-microtome (Leica). Sections were mounted on Superfrost Plus slides (VWR), dried at room temperature for at least 2 h, and stored at –20 °C until use. For BrdU analysis, the pregnant rat was injected subcutaneously with BrdU (100 mg/kgbw) 2 h prior to the sacrifice.

To define effects of CKIs on neuronal differentiation in vivo, cortices from each electroporated embryo were dissected individually 24 h or 48 h after in utero electroporation, incubated in trypsin solution for 15 min followed by trypsin inhibitor solution, and mechanically dissociated in Neurobasal/B27/bFGF medium. Cells were plated for 2 h on poly-D-lysine-coated dishes, fixed, and assessed for TuJ1 immunoreactivity.

Q-RT-PCR

Total RNA was extracted using the RNeasy Mini Kit (Qiagen). During RNA isolation, contaminating DNA was removed by DNase I treatment (Qiagen) according to manufacturer's instructions. One microgram of total RNA was reverse transcribed with SuperScript II reverse transcriptase (Invitrogen) in presence of random primers (Promega), dNTPs (Promega), and RNase inhibitor (RNaseOUT, Invitrogen). Quantitative PCR was performed on cDNA using the PCR Master Mix (Applied Biosystems) which contains buffer and preset concentrations of $MgCl_2$, dNTPs, and SYBRgreen in the presence of forward and reverse primers specific for the gene of interest (900 nM each). The primers, designed by using the Primer Express software (Applied Biosystems), were: p21 forward primer 5′-GACATCTCAGGGCCGAAAAC-3′, p21 reverse primer 5′-CGGCGCTTGGAGTGATAGAA-3′, p27 forward primer, 5′-CCTTCGACGCCAGACGTAAA-3′, p27 reverse primer 5′-AGCAGTGATGTATCTAATAAACAAGGAATT-3′, p57 forward primer, 5′-ACCCCGCGCAAACGT-3′, p57 reverse primer 5′-AGATGCCCAGCAAGTTCTCTCT-3′, Ngn2 forward primer 5′-ATTCTCGCCGGGTCTATTCAC-3′, Ngn2 reverse primer 5′-GCTGCCTGGCTGAAATGC-3′. PCRs were performed in the ABI Prism 7000 Sequence Detection system (Applied Biosystems). Amplifications obtained with rodent GAPDH forward and reverse primers (200 nM each) were used as reference (TaqMan Rodent GAPDH, Applied Biosystems). The relative differences between groups were calculated based on the values of the gene of interest normalized over the corresponding values of the GAPDH gene.

Western Blotting Analysis

Prior to analyzing p57 protein localization in embryonic cortex by immunohistochemistry, we assessed the specificity of 7 commercial anti-p57 antibodies by western blotting on cortex homogenates obtained from E14.5 WT and p57KO mouse embryos. Antibodies tested were from Sigma (KP39/P2735, mouse), Lab Vision-NeoMarkers (KP10/Ab-6/clone 57P06, mouse), BD-Pharmingen (#556346, mouse), and Santa-Cruz Biotechnology (C-20/sc-1040, rabbit; E-17/sc-1037, goat; H-91/sc-8298, rabbit; M-20/sc-1039, goat). Both the right and left cortices were dissected after removing the meninges, pooled, and then homogenized in the same lysis buffer, as described previously (Mairet-Coello et al. 2009). Briefly, lysates were sonicated, and the supernatants were assayed for protein content using the Bio-Rad Protein Assay (Bio-Rad). Eighty micrograms of protein were separated by sodium dodecyl sulfate–polyacrylamide gel electrophoresis and then electrotransferred onto polyvinylidene difluoride membranes (Bio-Rad). Membranes were blocked with blocking buffer containing 5% fat-free dry milk in Tris-buffered saline solution and Tween 20 (10 mM Tris–HCl pH 7.4, 150 mM NaCl, 0.05% Tween 20) and incubated overnight at 4 °C with primary antibody diluted in blocking buffer (1:20-1:2000). Incubations with horseradish peroxidase conjugated secondary antibodies (1:1000) were performed for 1 h at room temperature, and visualization was performed using chemiluminescence (ECL, Amersham Biosciences). While all the antibodies labeled p57 overexpressing cells after in vitro transfection (data not shown), only 2 (E-17/sc-1037 and H-91/sc-8298) revealed specific endogenous protein signal by western blotting, that is, a 57 kDa band in WT mouse cortex homogenates that was absent in p57KO cortex. Only the H-91/sc-8298 gave specific cellular labeling in embryonic mouse cortex by immunohistochemistry (see next section and Result section). p57 antibodies that were not specific based on western blotting also gave rise to cortical immunostaining localized to nuclei and/or cytoplasm in both the WT and p57KO embryos (data not shown).

Immunocytochemistry and Immunohistochemistry

Primary antibodies used in this study included antibodies to p27 (BD-Pharmingen #554069, mouse, 1:1000; Santa-Cruz sc-528/C-19, rabbit, 1:400), p57 (Santa-Cruz sc-8298/H-91, rabbit, 1:50 on mouse brain sections and 1:200 for overexpression studies; sc-1039/M-20, goat, 1:200 for detection of Cterp57), Ngn2 (Santa-Cruz sc-50402/H-55, rabbit, 1:50), S-phase marker BrdU (Becton-Dickinson Biosciences, mouse, 1:100), M phase marker phosphohistone H3 (Ser10, Upstate Biotechnology-Millipore, rabbit, 1:200), cell cycle marker PCNA (Santa-Cruz sc-25280, mouse, 1:1000), neural precursor marker nestin (Chemicon-Millipore, mouse, 1:400 for cell cultures, 1:1000 on tissue sections), early neuronal marker βIII-tubulin (TuJ1, Covance, rabbit or mouse, 1:1000), transcription factor Tbrain-1 (Tbr1, Chemicon-Millipore, rabbit, 1:2000 for cell cultures, 1:1000 for sections), astrocyte marker glial fibrillary acidic protein (GFAP, DakoCytomation, rabbit, 1:3000 for cell cultures, 1:500 on tissue sections), mature neuronal marker NeuN (Chemicon-Millipore, Mouse, 1:1000), GFP (Chemicon-Millipore, chicken, 1:500), Layer II-III marker Cux1 (anti-CDP M-222, Santa Cruz sc-13024, rabbit 1:200), apoptotic marker activated caspase-3 (Cell Signaling, Asp175, rabbit, 1:200). Cells or sections were rinsed in PBS containing 0.3% triton X-100 (PBS-T) for 10 min and incubated with the primary antibody overnight at 4 °C. Monoclonal antibodies were diluted in PBS-T, and polyclonal antibodies were diluted in a PBS-T solution containing 10% lactoproteins, 1% bovine serum albumin, and 0.01% sodium azide. Staining was visualized using Alexa Fluor 588 (1:500-1:1000), 594 (1:500-1:1000), or 350 (1:200-1:400) conjugated secondary antibodies (Molecular Probes-Invitrogen).

For p57 and p27 immunodetection in embryonic mouse neocortex, brains were dissected and fixed by immersion in 1% PFA-PBS for 1 h at 4 °C and incubated in 30% sucrose-PBS overnight at 4 °C. Brains were embedded and cryo-sectioned as described above (see In Utero Electroporation section). For BrdU detection, cells and sections were treated prior to immunolabeling with 50 U/mL (cell cultures) or 500 U/mL (tissue sections) DNase I for 10 min at room temperature (Ye et al. 2007). For NeuN and Cux1 detection, sections were submitted to antigen retrieval procedure in 10 mM citrate buffer pH = 6 at 90 °C for 5 min.

Acquisition and Treatment of Microscope Images

Cells in culture were examined with an inverted fluorescence microscope (Axiovert 200M, Carl Zeiss MicroImaging) under control of AxioVision software 4.5 (Carl Zeiss MicroImaging). Images were acquired under fluorescence or phase optics using ×20 or ×40 NeoFluar objectives. Images of brain sections were obtained with a Zeiss LSM 510 laser scanning confocal microscope (Carl Zeiss MicroImaging) equipped with ×10, ×25, and ×63 objectives, under control of LSM 510 meta software. Figures were produced using Adobe Photoshop software with minimal alteration of captured images.

Cell Counting and Data Analysis

For in vitro studies of cell differentiation, transfected rat cells (EGFP autofluorescence) immunolabeled with the indicated marker were counted at ×20 objective in 10 nonoverlapping fields on at least 3 coverslips per group (400–1000 cells/vector) from 3 independent experiments, using AxioVision 4.5 software. Number of WT and p57KO mouse cortical cells labeled for nestin and TuJ1 were counted at ×20 objective in 10 nonoverlapping fields on two 35-mm dishes per embryo (WT: n = 10 embryos, p57KO: n = 8 embryos, 3 litters, 2000–2500 cells), using AxioVision 4.5 software. The smallest cell body diameter and length of the longest process visualized with EGFP autofluorescence were measured at ×20 objective, on 5–10 randomly selected fields, on 3 coverslips per group (100–150 cells/vector), using the measurement function of Image Pro Plus 6.0 Software (Media Cybernetics). The number of cells bearing at least one process longer than 5 cell body diameters was quantified based on these measurements. Analysis of processes in E14.5 WT and p57KO mouse cortical cells was performed using an Axiovert 35 microscope (Carl Zeiss MicroImaging), directly under a ×32 objective of a brightfield phase microscope. The number of cells bearing at least one process greater than 2 cell body diameters was counted in three 1-cm rows on two 35-mm dishes per embryo (300–400 cells/dish, 3 embryos/genotype). Process length of nestin+ and TuJ1+ cortical cells from WT and p57KO mice were measured at ×20 objective in 5 non-overlapping fields on one 35-mm dish per embryo (WT: n = 5 embryos, p57KO: n = 4 embryos, 80–120 cells), using Image Pro Plus 6.0 Software.

To study the potential relationship between protein expression levels and process outgrowth, the quantity of CKI overexpressed protein was evaluated by thresholding immunofluorescence using the Image Pro Plus software. Digital images were obtained with a Zeiss

Axiovert-200 microscope at ×20 objective using Axiovision software and a fixed exposure time that was below the threshold of saturation. The mean of intensity of p27 or p57 immunolabeling was measured in transfected cells inside an area delimited by the cell body. The length of the longest process was measured based on EGFP autofluorescence. Analyses were performed in 5 nonoverlapping fields on 2 coverslips (n = 50–60 cells/vector).

For in vivo study of differentiation, cortical cells were dissociated from 3 to 5 embryos per vector (from 4 different gestational injections), 24 h after in utero electroporation. βIII-tubulin+ EGFP+ cells were counted at ×20 objective in 12–14 nonoverlapping fields, using the Axiovert 200M microscope and AxioVision 4.5 software. For in vivo BrdU and cell migration analyses, 3–5 electroporated embryos were analyzed per group, using confocal microscopy and Image Pro Plus Software 6.0. The different zones of the embryonic cortex were identified with propidium iodide staining (Sigma) which reveals differences in cell densities, with high density in the VZ/SVZ, low density in the intermediate zone (IZ), and high density in the cortical plate (CP). BrdU labeling was analyzed in EGFP+ cells present in the VZ/SVZ, 24 h after electroporation. In order to detect changes of migration inside the CP, the CP was divided into 2 zones (upper and lower CP) with equivalent height. The number of EGFP+ cells was counted in the different cortical zones within a rectangle of 400-μm width, 3 or 4 days after electroporation and presented as the percent of EGFP+ cells counted per zone over the total number of EGFP+ cells counted in the rectangle. To study the potential relationship between protein expression levels and distance of migration, the quantity of CKI overexpressed protein was evaluated by thresholding immunofluorescence using Image Pro Plus. Digital images were obtained with a confocal microscope at ×25 objective and a fixed exposure time below the threshold of saturation. The distance of cell migration was measured from the wall of the LV. Analyses were performed on one representative section (n = 90–120 cells/vector).

For postnatal studies of neuronal and glial fate, sections of P10 brains electroporated at E15.5 or E18.5 were triple labeled for NeuN, GFAP, and GFP. The proportion of EGFP+ cells expressing NeuN or GFAP was counted on 4 sections per brain from 4 to 7 pups per group using Z-stack function of Axiovert 200M microscope equipped with Apotome and Axiovision software. For radial migration analyses at P10 of brains electroporated at E15.5, the radial extent of the cortical wall was divided into 9 bins of equivalent height from layer VI to II. To study cell positioning within the cortical layers II–III, P10 brain sections were labeled for Cux1, a specific marker of layers II-III. Layers labeled for Cux1 were divided into 2 equal bins. The proportion of EGFP+ cells was counted in the different bins within a rectangle of 600-μm width on 2 sections per brain (4–7 pups per group) using Image Pro Plus software.

All data are expressed as means ± standard error of the mean (SEM). Statistical analyses were performed using the one-way analysis of variance followed by Dunnett post hoc test to compare multiple groups with control (GraphPad InStat 3). When indicated, unpaired Student's t test (2-tailed P value) was used to compare 2 groups.

Results

p57 Is Expressed in Both Proliferative and Postmitotic Compartments in the Developing Cortex

To first define the temporal relationships of the CKIs in the cortex, we examined expression of p21, p27, and p57 mRNAs in developing rat cortex using Q-RT-PCR. All 3 genes are expressed throughout corticogenesis but exhibit distinct temporal profiles. The level of p21 expression increases gradually from E12.5 to E20.5. p27 mRNA was abundant at mid- and late-corticogenesis, while p57 was more abundantly expressed at early and middle stages (Fig. 1*A*), suggesting that Cip/Kip members may play distinct roles at different stages of cortical development. Moreover, in agreement with previous studies (van Lookeren Campagne and Gill 1998), PCR amplification profiles suggest that p21 is weakly expressed in developing embryonic cortex in comparison with p27 and p57 (not shown), suggesting that p21 does not likely exert a dominant role during cortical development. We thus focused our analyses on p57 and p27.

To begin exploring the role of p57 and p27 in corticogenesis, we examined their expression in the cerebral cortex of E14.5 mouse embryos by immunohistochemistry. p57 was localized in nuclei of postmitotic cells of the CP and migrating cells of the IZ as well as cells in the proliferative zones (Fig. 1*B*), whereas p27 expressing cells were primarily found in the IZ and CP with fewer cells in the VZ/SVZ (Fig. 1*D*). In the VZ/SVZ, p57 was expressed in a group of proliferating precursors and as well as postmitotic neurons, as shown by coexpression with cell cycle marker PCNA and early neuronal marker βIII-tubulin, respectively (Fig. 1*F,G*). The specificity of the p57 antibody was assessed by western blotting on protein extracts from E14.5 WT and p57KO mouse cortices. While a strong 57 kDa band was detected in WT cortex, only a weak signal was noted in p57KO cortex (Supplementary Fig. S1). Moreover, no p57 immunoreactivity was detected on p57KO brain sections, confirming that the antibody does not cross-react with the other Cip/Kip members (Fig. 1*C*). For p27 immunodetection, we used 2 different antibodies and found that both exhibited the same pattern of expression on WT mouse cortical sections. In contrast, no p27 signal was detected in p27KO brains, indicating the specificity of the antibodies (Fig. 1*E* and not shown).

These observations indicate that expression of p57 coincides with the transition from precursor cell to postmitotic neuron, suggesting p57 may play roles at different steps of neurogenesis, including cell cycle control, migration, and differentiation. Similar roles were previously reported for p27 (Nguyen et al. 2006).

p57 Expression Is Regulated by Mitogenic and Differentiation Factors in Embryonic Cortical Precursors

To examine p57 regulation during cortical development, we analyzed its expression by Q-RT-PCR in cultures of E14.5 rat cortical precursors incubated in serum-free defined medium (Lu and DiCicco-Bloom 1997) following exposure to factors controlling proliferation and/or differentiation. We analyzed p27 expression in parallel to determine whether p57 and p27 genes exhibit distinct or similar regulation. Moreover, to explore possible relationships with genes involved in neurogenesis, we examined expression of pro-neural bHLH transcription factor Ngn2.

In the presence of mitogenic signal bFGF, levels of both p57 and p27 mRNAs were decreased in E14.5 cortical precursor cultures at 24 h (p27: 44.3 ± 2.70%; p57: 44.4 ± 3.69%; mean % ± SEM, normalized to GAPDH and expressed as % of control considered as 100%; n = 6; $P < 0.001$), supporting their role as negative regulators of the cell cycle (Sherr and Roberts 1999). Ngn2 mRNA level was also decreased by the mitogenic factor (13.3 ± 0.67% of control; n = 6; $P < 0.01$). Conversely, when neuronal differentiation was induced by bFGF withdrawal 24 h after plating, p57, p27, and Ngn2 mRNA levels were all increased, by 26%, 52%, and 96%, respectively, 24 h later ($P < 0.05$; $P < 0.01$; $P < 0.01$; n = 6). However, when differentiation was triggered by antimitogenic/differentiation factor PACAP, only p57 and Ngn2 mRNA levels were increased at 24 h, with no change in p27 expression

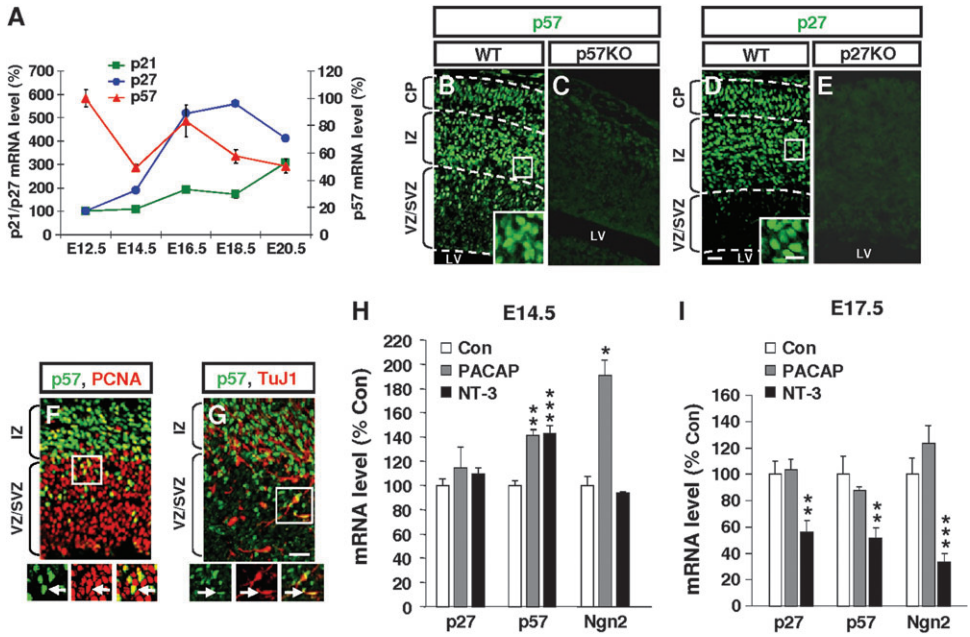

Figure 1. CKI expression in developing rat cerebral cortex and regulation by differentiation factors in vitro. (*A*) Temporal patterns of CKI gene expression in developing rat cortex. Total RNA was extracted from cortices at the indicated stages of embryonic development and was subjected to Q-RT-PCR analysis. Data represent means ± SEM of values normalized to GAPDH and expressed as the percentage of the mRNA level at E12.5 (considered as 100%). p21 expression increases gradually from E12.5 to E20.5. While p27 exhibits major expression during mid- to late-corticogenesis, p57 mRNA is more abundant at early and middle stages. $n = 3$ embryos. (*B–D*) p57 and p27 immunolabeling on frontal sections of E14.5 mouse neocortex. p57 (*B*) and p27 (*D*) are expressed mainly in the CP and IZ and in a subset of cells in the proliferative regions (VZ/SVZ). p57 and p27 signals were virtually absent in the cortex of p57KO (*C*) and p27KO (*E*) mouse, respectively, confirming the specificity of the labeling. Insets in *B* and *D* show the predominant nuclear localization of both p57 and p27 proteins. (*F*, *G*) In the VZ/SVZ, p57 was expressed in both cycling (PCNA+, *F*) and postmitotic (TuJ1+, *G*) cells. (*H*, *I*) Cultures of E14.5 (*H*) or E17.5 (*I*) rat cortical precursors were incubated with differentiation factors PACAP (10^{-8} M) or NT-3 (10 ng/mL) for 24 h. At 24 h, total RNA was extracted and submitted to Q-RT-PCR analysis. Values were normalized to GAPDH and expressed as percent of control (means ± SEM). At E14.5, PACAP increased p57 and Ngn2 mRNA levels while NT-3 only increased p57 expression. At E17.5, PACAP had no effect on CKI or Ngn2 mRNA levels while NT-3 decreased p27, p57, and Ngn2 expression. $n = 6$ dishes, 3 experiments, $^*P < 0.05$, $^{**}P < 0.01$, $^{***}P < 0.001$, using unpaired Student's *t* test. Scale bars: 25 μm (*B–G*).

(Fig. 1*H*). Finally, expression of p57 only was increased by NT-3 (Fig. 1*H*). These results suggest that during the early-middle period of neurogenesis, p57 plays a role in neuronal differentiation and exhibits distinct regulation, consistent with its ontogenetic expression (Fig. 1*A*).

In addition to differential regulation at E14.5, we wondered whether the CKIs may exhibit stage-dependent responses. Thus, we examined their expression in E17.5 rat cortical cells treated with PACAP or NT-3. p57, p27, and Ngn2 mRNA levels were not affected in E17.5 cortical cells incubated with PACAP for 24 h (Fig. 1*I*) while S-phase entry, measured by the incorporation of ^{3}H thymidine (Lu and DiCicco-Bloom 1997; Mairet-Coello et al. 2009), was decreased (34.8 ± 4.13% of vehicle; $n = 4$; $P < 0.001$). These results suggest that 1) p57 regulation by PACAP is developmental stage-specific, 2) p27 is not transcriptionally regulated by PACAP, and 3) the antimitogenic effect of PACAP is mediated through different pathways at early and late embryonic stages. Surprisingly, NT-3 decreased p57, p27, and Ngn2 mRNA levels in E17.5 cells (Fig. 1*I*). In this condition, S-phase entry was unexpectedly increased (192 ± 2.15% of control; $n = 4$; $P < 0.001$), suggesting that NT-3 has a mitogenic and/or trophic activity on cortical precursors at this embryonic stage.

Altogether, these results indicate that p57 and p27 expression are 1) differentially regulated by differentiation factors and 2) their regulation depends on the developmental stage.

p57 Promotes Cell Cycle Exit of Cortical Precursors In Vitro Via Its N-terminal Domain, While Its C-terminal Portion Stimulates Proliferation

To further explore the roles of p57 in corticogenesis, we used overexpression strategies: E14.5 rat cortical precursors were transfected with bi-cistronic expression plasmids containing EGFP and p57 cDNAs and assessed for proliferation and differentiation markers. Effects of p57 were compared with those of p27 and Ngn2 that induce neuronal differentiation in cortical precursors (Ge et al. 2006; Nguyen et al. 2006).

Before examining effects of vector overexpression on cortical precursors in culture, we characterized cell composition of the model system. E14.5 cells were plated on poly-D-lysine and laminin-coated coverslips and incubated in Neurobasal/B27/bFGF medium for 2 h. Cells were fixed and processed for nestin and βIII-tubulin immunostaining. While 78% (±1.65; $n = 3$ coverslips) of cells expressed nestin, 15% (±2.02; $n = 3$ coverslips) expressed βIII-tubulin only, suggesting that the majority of cells at the time of transfection were initially precursors. Furthermore, the efficacies of plasmid constructs and transfections were verified by immunocytochemistry using antibodies against p57, p27, and Ngn2. High levels of the corresponding proteins were produced in cells transfected with the constructs (Supplementary Fig. S2*A–O*). Moreover, all plasmids lead to similar transfection efficiencies (Supplementary Fig. S2*P*). Finally, to assess possible changes in

survival, we examined colocalization of apoptotic marker activated caspase 3 and found that it was similar for all constructs (Supplementary Fig. S2*Q*–*T*).

We first determined whether overexpressed CKI proteins were functional in cell cycle regulation by analyzing nuclear incorporation of S-phase marker BrdU. The proportion of p57 and p27 transfected cells entering S-phase was strongly reduced at 24 h by overexpressed CKIs (EGFP: 15.2 ± 1.18%; p27: 1.39 ± 0.27%; p57: 1.58 ± 0.19%; $P < 0.01$) and 48 h (Fig. 2*A*–*C*), indicating that p57 and p27 overexpression induces cell cycle arrest. Ngn2 also elicited cell cycle exit but not as effectively as the CKIs (Fig. 2*A*).

In previous studies of p27, the highly conserved N-terminal domain alone regulated cell cycle inhibition but also promoted neural differentiation (Ohnuma et al. 1999; Nguyen et al. 2006). Thus, we analyzed the effects of overexpressing the N-terminal portion of p57 (Nterp57) that contains the cyclin/CDK binding/inhibitory domains and compared it with the C-terminal portion of p57 (Cterp57) that contains unique proline and acidic domains not shared by other Cip/Kip family members (Nakayama 1998). Similar to full-length p57, transfection with the Nterp57 construct strongly reduced BrdU incorporation, while in marked contrast, Cterp57 increased the percent of cells incorporating BrdU (Fig. 2*A*). Furthermore, Cterp57 overexpression also increased mitosis at 48 h since more cells expressed the M-phase marker phosphohistone H3 (EGFP: 15.0 ± 1.64%; Cterp57: 24.5 ± 1.57%; $P < 0.05$). Together, these results indicate that 1) the N-terminal part of p57 is necessary and sufficient to elicit cell cycle exit and 2) Cterp57 portion stimulates proliferation.

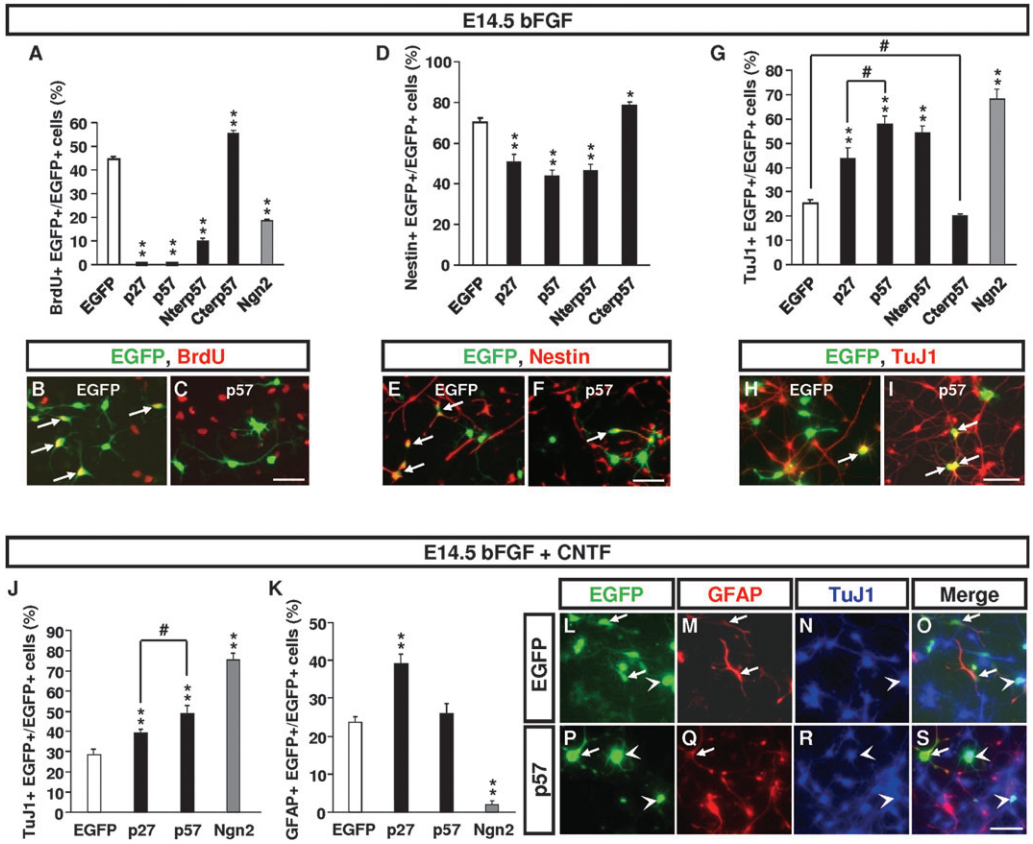

Figure 2. Effects of p57 and p27 overexpression on cell cycle progression and differentiation of E14.5 cortical precursors in vitro. (*A*–*I*) E14.5 rat cortical cells incubated in standard defined medium containing bFGF (10 ng/mL; see Materials and Methods) were transfected with the indicated plasmids 2 h after plating. Cells were fixed at 48 h and processed for immunostaining. Some cultures were incubated with BrdU for the last 4 h of culture. The number of EGFP+ cells labeled for BrdU, nestin, or TuJ1 was counted in 10 randomly selected fields. (*A*) The proportion of cells incorporating BrdU was strongly reduced at 48 h in p27, p57, and Nterp57 overexpressing cells compared with cells transfected with the empty EGFP plasmid. Ngn2 transfection also reduced BrdU incorporation but not as effectively as CKIs. In contrast, overexpression of Cterp57 increased BrdU incorporation. (*B*, *C*) Double labeling for EGFP (green) and BrdU (red) 48 h after transfection with EGFP control (*B*) or p57 (*C*) plasmids. Arrows identify double-labeled cells. (*D*) The proportion of cells expressing precursor marker nestin was decreased after p27, p57, and Nterp57 transfection but increased in cells transfected with Cterp57. (*E*, *F*) Double immunolabeling for EGFP (green) and nestin (red) in cells transfected with the empty EGFP plasmid (*E*) or p57 (*F*) vector. (*G*) The percent of cells labeled for neuronal marker TuJ1 was increased after p27, p57, and Nterp57 transfection and decreased in Cterp57 transfected cells. Some cultures were transfected with proneural Ngn2 plasmid, whose overexpression strongly promoted neuronal differentiation. (*H*, *I*) Double labeling for EGFP (green) and TuJ1 (red) after transfection with control (*H*) or p57 (*I*) plasmids. (*J*–*S*) After transfection, E14.5 cortical cells were incubated in medium containing bFGF (10 ng/mL) and CNTF (10 ng/mL) for 48 h to promote astroglial differentiation. The percentage of cells labeled for neuronal marker TuJ1 still increased after p27 and p57 overexpression in an astrocyte-promoting environment (*J*). More p27-transfected cells exhibited astrocyte marker GFAP, whereas the proportion of GFAP+ cells in p57 overexpressing cells was similar to the control (*K*). While a majority of cells transfected with Ngn2 were TuJ1+ (*J*), virtually no cells displayed GFAP expression (*K*). (*L*–*S*) Triple immunostaining for EGFP (green), GFAP (red), and TuJ1 (blue) after transfection with the empty (*L*–*O*) or p57 (*P*–*S*) vector. Arrows show colocalization of EGFP and GFAP expression and arrowheads identify EGFP+ TuJ1+ double-labeled cells. In all graphs, error bars indicate SEM ($n = 3$–8 coverslips/group, 3 experiments, 400–700 EGFP+ cells, $*P < 0.05$, $**P < 0.01$, using the one-way analysis of variance followed by Dunnett post hoc test; $\#P < 0.05$, using unpaired Student's *t* test). Scale bars: 50 μm (*B*, *C*, *E*, *F*, *H*, *I*, *L*–*S*).

p57 and p27 Both Promote Precocious Neuronal Differentiation

To compare effects of p57 and p27 on neuronal differentiation, cells transfected with CKI plasmids were immunolabeled for precursor marker nestin, postmitotic transcription factor Tbr1, or early neuronal marker βIII-tubulin at 48 h. The proportion of nestin+ precursors was decreased in p27 and p57 transfected cells (Fig. 2*D–F*), indicating that fewer cells were precursors after CKI overexpression. Conversely, the percentages of Tbr1+ (Supplementary Fig. S3*A–D*) and βIII-tubulin+ neurons (Fig. 2*G–I*) were both increased in p27 and p57 overexpressing cells, suggesting that both CKIs promote the transition from proliferation to differentiation. Interestingly, the increases elicited by p57 in both neuronal markers were approximately twice that resulting from p27 overexpression. For example, p57 overexpression increased the proportion of TuJ1-expressing cells to 58% compared with 28% in EGFP control (Fig. 2*G*; a 107% increase), whereas p27 only increased TuJ1 expression to 43%, representing a 56% increase. The greater stimulatory effects on TuJ1 and Tbr1 of p57 compared with p27 suggest potential differential effects on neuronal differentiation. By comparison, the neurogenic effects of p27 and p57 were somewhat smaller than the effect of Ngn2 (Fig. 2*G*).

To define potential structural–functional relationships, we analyzed neural markers after transfecting the N- and C-terminal halves of p57. Nterp57 overexpression reduced neural precursors (Fig. 2*D*) and induced neuronal differentiation as efficiently as full-length protein (Fig. 2*G*, Supplementary Fig. S3*A,B, E*) suggesting that the N-terminal part of p57 alone, like the N-terminal part of p27 (Nguyen et al. 2006), is sufficient to induce neuronal differentiation. In contrast, the proportion of nestin-expressing progenitors increased after Cterp57 transfection (Fig. 2*D*) while the percentage of differentiated neurons was reduced (Fig. 2*G*, Supplementary Fig. S3*A,B,F*). This apparent reduction in differentiation markers probably reflects the increased number of dividing cells observed after Cterp57 transfection (Fig. 2*A*).

Complementary experiments using loss of function approaches were performed previously to investigate the roles of CKIs in cortical differentiation (Nguyen et al. 2006; Itoh et al. 2007). To extend this work, we analyzed neuronal differentiation in vitro of E14.5 mouse embryonic cortical precursors that were deficient for p57. After 48 h of culture, we observed a phenotype opposite to that we observed in the overexpression model: the percent of precursors expressing nestin increased while the proportion of cells labeled for βIII-tubulin was reduced in p57KO cortical cells in comparison with WT cells (Fig. 3*A–D*), indicating that the balance between precursors and differentiated neurons was altered in the absence of p57.

In aggregate, these results suggest that both p57 and p27 participate in the switch from cortical progenitor proliferation to neuronal differentiation, consistent with their expression pattern in the isocortex (Fig. 1*B,D*).

p57 and p27 Regulate Neuronal/Glial Cell Fate in a Context-Dependent Manner

The foregoing data indicate that overexpression of both p57 and p27 promotes precocious neuronal differentiation. To explore whether CKIs might influence neuronal versus glial cell fate, we challenged cells transfected with CKIs by

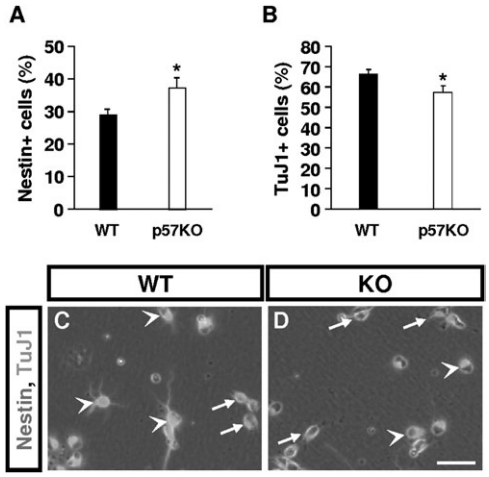

Figure 3. Neuronal differentiation of p57KO cortical precursors in vitro. Cortical cells from E14.5 WT and p57KO mice were cultured for 48 h on poly-D-lysine-coated dishes, fixed, and processed for nestin and TuJ1 double immunolabeling. (*A*, *B*) The number of nestin+ cells and TuJ1+ cells were counted in 10 nonoverlapping fields on 2 dishes per embryo. While the proportion of nestin+ cells was increased in p57KO cortex (*A*), the proportion of TuJ1+ cells was decreased (*B*). Data represent means ± SEM (n = 8–10 embryos, 3 litters). (*C*, *D*) Double fluorescence images for nestin (red, arrows) and TuJ1 (green, arrowheads) were merged with phase microscopy. $^*P < 0.05$, using unpaired Student's t test. Scale bar: 50 μm (*C*, *D*).

providing a factor known to promote astrogliogenesis, CNTF (Bonni et al. 1997). We retained bFGF in the posttransfection medium as the factor enhances CNTF-mediated astrocyte differentiation (Song and Ghosh 2004). In these conditions, p57 and p27 were as effective in promoting cell cycle exit at 48 h as in medium containing bFGF only, as indicated by BrdU labeling index (EGFP: 39.8 ± 0.93%; p27: 1.2 ± 0.23%; p57: 1.1 ± 0.19%; $P < 0.01$). Moreover, p57 and p27 both increased the proportion of βIII-tubulin+ cells (Fig. 2*J*). The effects, though somewhat smaller, reproduced the advantage in neuronal differentiation elicited by p57 (Fig. 2*G*).

To examine gliogenesis, we characterized cells for astroglial marker GFAP. No GFAP immunoreactivity was detected at 2 days in cultures incubated with bFGF only (data not shown), consistent with our previous report (Carey et al. 2002) and the notion that neurogenesis is predominant at this time (Bonni et al. 1997; Sun et al. 2001). In the presence of CNTF, 23% of cells transfected with the empty EGFP plasmid expressed GFAP at 48 h (Fig. 2*K–O*). In cells overexpressing p27, the percent of GFAP+ cells was strongly increased (Fig. 2*K*), while in contrast, there was no change in the percent of cells expressing GFAP following p57 overexpression (Fig. 2*K–S*). These observations suggest that CNTF can promote astrocyte differentiation in additional cells in the presence of p27, whereas p57 overexpression is not permissive for glial differentiation induced by CNTF. By comparison, Ngn2 overexpression enhanced neuronal differentiation as efficiently as in the medium without CNTF (Fig. 2*J*). More strikingly, Ngn2 prevented the glial cell fate, reducing GFAP expression (Fig. 2*K*).

To determine whether cell response to CKI overexpression depends upon the developmental stage of the progenitors, we performed similar experiments with cortical cells isolated from a later embryonic stage, E17.5. In the presence of bFGF alone, p57 and p27 overexpression increased neuronal differentiation of E17.5 cortical cells and reproduced the differential effects observed at E14.5 (Fig. 4*A*). p57 and p27 also markedly

increased the proportion of E17.5 cells expressing GFAP by 6.5- and 10-fold, respectively (Fig. 4*B*), indicating that at a later embryonic stage, the 2 CKIs elicit precocious differentiation of both neuronal and glial progenitors. However, p57 overexpression produces proportionally more neurons than astrocytes while p27 favors gliogenesis, suggesting that CKIs may bias progenitors toward one lineage. Thus, we challenged E17.5 cortical precursors with astrogliogenic factor CNTF. In the presence of CNTF, p57 and p27 overexpression still increased neuronal differentiation of E17.5 cortical cells, by 3.3- and 2.2-fold, respectively (Fig. 4*C*). The response of E17.5 cells to CNTF, however, was greater than E14.5 cells (Fig. 2*K*), with 65% of cells transfected with the control vector expressing GFAP (Fig. 4*D*). Contrary to E14.5 cells, p27 transfection did not enhance astrocyte differentiation elicited by CNTF while p57 decreased the proportion of GFAP+ cells, suggesting that p57 may partially prevent the astroglial fate promoted by CNTF in E17.5 precursors (Fig. 4*D*). Similar to E14.5 cells, Ngn2 overexpression promoted neuronal differentiation and prevented CNTF astrogliogenic effects in E17.5 cells, increasing the proportion of βIII-tubulin+ cells by 4.7-fold (Fig. 4*C*) and reducing GFAP expression (Fig. 4*D*).

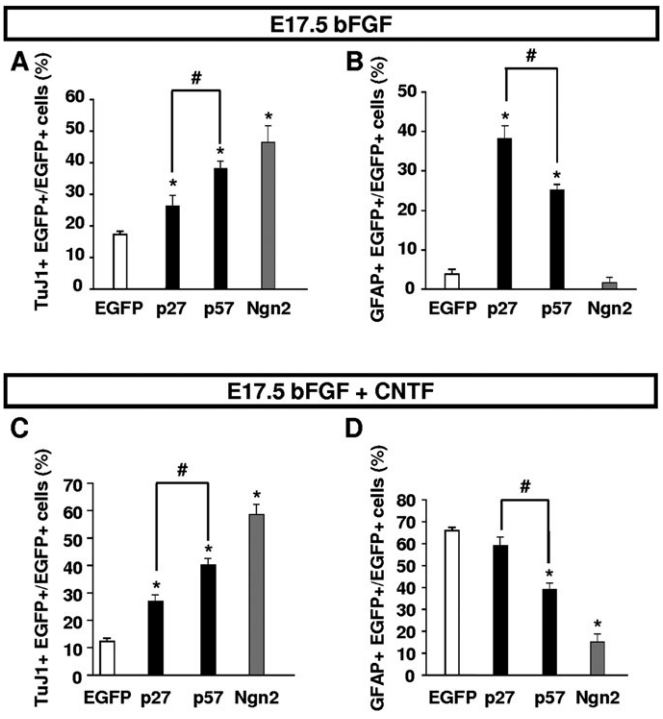

Figure 4. Effects of p57 and p27 overexpression on cell differentiation of E17.5 cortical precursors in vitro. E17.5 cortical cells were transfected with the indicated vector 2 h after plating and incubated in medium containing bFGF only (10 ng/mL, *A*, *B*) or bFGF plus CNTF (10 ng/mL, *C*, *D*) for 48 h. (*A*, *B*) In medium containing bFGF only, overexpression of both p27 and p57 increased the proportion of TuJ1+ (*A*) as well as GFAP+ (*B*) cells while Ngn2 selectively increased the proportion of TuJ1+ cells. (*C*, *D*) In presence of CNTF, p27, p57, and Ngn2 still increased the proportion of TuJ1+ cells (*C*). GFAP expression (*D*) was strongly increased in control cells. While p27 overexpression did not significantly affect GFAP expression, less p57 transfected cells exhibited GFAP signal compared with the control. Ngn2 overexpressing cells were weakly responsive to astrogliogenic effect. In all graphs, error bars indicate SEM (n = 3–8 coverslips/group, 3 experiments, 400–700 EGFP+ cells, $^*P < 0.01$, using the one-way analysis of variance followed by Dunnett post hoc test; $\#P < 0.05$, using unpaired Student's t test).

In aggregate, these results suggest than p57 and p27 differentially modulate neuronal and glial differentiation depending upon the developmental stage of the progenitors and the environmental signals. In contrast, Ngn2 can instruct neuronal cell fate regardless the developmental stage or extracellular signals.

CKI Overexpression Enhances Process Outgrowth of Cortical Precursors In Vitro

Since cell cycle exit is correlated with neuritogenesis (Perez-Martinez and Jaworski 2005; Song et al. 2005), we examined whether CKIs also affect process outgrowth. We counted the number of processes per cell and measured the length of the longest process at 48 h after transfection. We found that the average number of primary processes per cell was significantly higher in p57 and p27 transfected cells (EGFP: 1.35 ± 0.14; p27: 2.55 ± 0.12; p57: 3.14 ± 0.36; mean number of processes ± SEM; $P < 0.05$). The average length of the longest process was markedly increased in p57 and p27 overexpressing cells (Fig. 5*A*). Moreover, about twice as many p57 transfected cells extended very long processes (≥5 cell body) compared with p27 and 4 times as many compared with control (Fig. 5*B–E,H*), suggesting that CKIs may differentially regulate process outgrowth.

To extend the analysis of p57 structure–function relationships, we also examined process outgrowth in Nterp57 and Cterp57 transfected cells. While transfection of cells with Nterp57 promoted process outgrowth comparable with full-length p57 (Fig. 5*A–C,E,F*), cells transfected with Cterp57 did not exhibit longer processes compared with EGFP group (Fig. 5*A–C,G*).

Since the quantity of plasmids integrated in a cell or the amount of protein translated cannot be controlled during transfection, we considered the possibility that differences in CKI-induced process outgrowth may be a consequence of differences in protein expression levels. We thus asked whether there was a relationship between the quantity of protein overexpressed in a cell and process length. Our observations show no correlation between the protein amount and process length, indicating that the differential effects of p57 and p27 on process outgrowth are not due to differences in protein levels (Supplementary Fig. S4*A,B*). In addition, we measured process length in cells transfected with 3 different initial quantities of plasmids. We found that 1) cell process length was not modified by the plasmid concentration used for a given vector and 2) p57 and p27 had differential effects on process outgrowth regardless of the initial plasmid concentration used for transfection (Supplementary Fig. S4*C*).

Although unlikely, we also considered the possibility that differences in CKI effects on process outgrowth resulted from the effects of chemical transfection reagents on process attachment or elongation. To address this, we introduced plasmids into E15.5 rat brains by ex vivo transuterine intracerebroventricular injections followed by electroporation. Cortical cells were immediately dissociated and cultured for 48 h on poly-D-lysine and laminin-coated glass coverslips in Neurobasal/B27/bFGF medium: We observed similar effects of p57 and p27 overexpression by electroporation on process outgrowth (Supplementary Fig. S4*D–F*).

To define the relationship of process extension to developmental stage of the precursor, we analyzed process

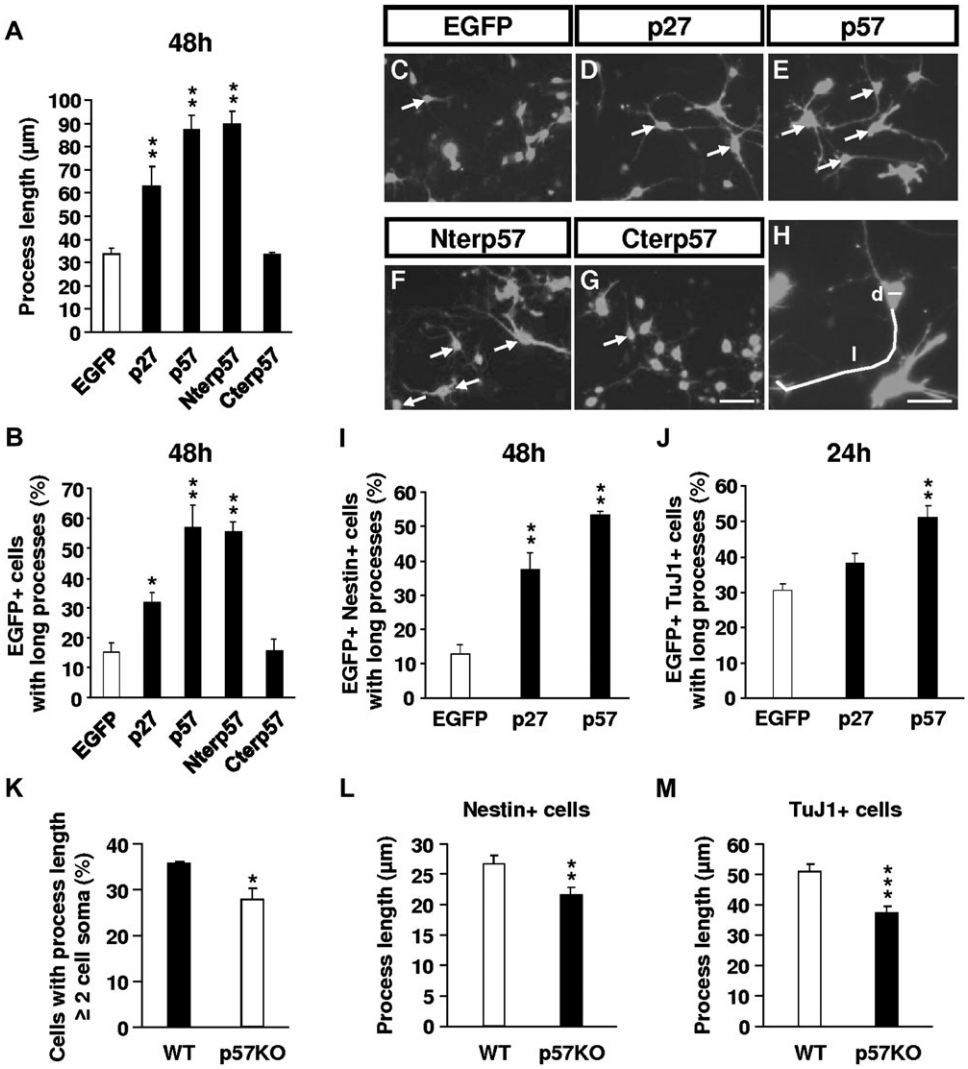

Figure 5. *(A–J)* Effects of p57 and p27 overexpression on process outgrowth of E14.5 rat cortical precursors in vitro. The smallest cell body diameter (d) and the length of the longest process (l) of EGFP+ cells were measured 48 h after transfection by tracing as shown in *H*. More than 100 cells were examined on at least 3 coverslips per group (3 independent experiments). (*A*) p27, p57, and Nterp57 overexpressing cells extended longer processes than control transfected cells. (*B*) Percentages of EGFP+ cells bearing at least one process with a length greater than 5 cell body diameters. More p57 and Nterp57 overexpressing cells extended very long processes compared with cells transfected with p27, control or Cterp57. (*C–H*) Illustrations of morphology of cells transfected with EGFP control (*C*), p27 (*D*), p57 (*E*), Nterp57 (*F*), or Cterp57 (*G*). Arrows identify EGFP+ cells with processes >5 cell body. *H* is a magnification of one of the p57 transfected cell in *E*. (*I*) The number of cells with long processes (≥5 cell body) was counted in nestin+ precursors at 48 h. More nestin+ cells extended long processes after p27 or p57 transfection. (*J*) The number of cells with processes ≥5 cell body were counted in cells expressing TuJ1 at 24 h. More TuJ1+ cells displayed a long process after p57 transfection. (*K*) The number of cells bearing at least one process greater than 2 cell body diameters was counted in E14.5 WT and p57KO mouse cells 24 h after plating, in three 1-cm rows on two 35-mm dishes per embryo (300–400 cells/dish, 3 embryos/genotype). The proportion of cells bearing a long process was reduced in p57KO cells compared with WT cells. (*L*, *M*) The length of the longest process was measured in nestin+ (*L*) and TuJ1+ (*M*) WT and p57KO cells 48 h after plating. Process length was reduced in both nestin+ (*L*) and TuJ1+ (*M*) p57KO cells compared with WT cells. Data represent means ± SEM, $*P < 0.05$, $**P < 0.01$, $***P < 0.001$. Scale bars: 50 μm (*C–G*), 25 μm (*H*).

outgrowth after in vitro transfection in both nestin+ precursors and βIII-tubulin+ cells. The percent of nestin+ precursors bearing processes with length greater than 5 cell body diameters was 4-fold higher after p57 transfection and 3-fold higher in p27 overexpressing cells compared with the control at 48 h (Fig. 5*I*). In contrast, the percentage of βIII-tubulin+ cells with long processes was not different at 48 h (EGFP: 80.1 ± 5.89%; p27: 86.5 ± 8.57%; p57: 81.3 ± 3.71%; $P > 0.05$). Nor was there any difference in the length of the longest processes (EGFP: 92.1 ± 0.43 μm; p27: 103.7 ± 14.41 μm; p57: 95.2 ± 2.55 μm; $P > 0.05$). Since the majority of βIII-tubulin+ cells extended processes with similar length by 48 h in all groups, suggesting a ceiling effect, we examined cells at an earlier time. At 24 h, more p57 overexpressing cells labeled for βIII-tubulin bore long processes (>5 cell body) compared with cells transfected with empty vector and p27 (Fig. 5*J*). These findings suggest that CKIs differentially regulate process outgrowth in both nestin+ precursors as well as differentiating neurons exhibiting βIII-tubulin.

Since p57 overexpression enhanced process outgrowth, we wondered whether the effect might be diminished in its absence. We examined process outgrowth in p57KO and WT mouse cortical cells in culture. The number of cells bearing processes (≥2 cell soma) was reduced in the p57-deficient cells compared with WT cells at 24 h (Fig. 5*K*). Since p57 overexpression increased process length in both neural

precursors and postmitotic neurons, we also measured process length of nestin+ progenitors and βIII-tubulin+ neurons in p57KO cortical cells. The length of the processes was reduced in both nestin+ (Fig. 5*L*) and βIII-tubulin+ p57KO cells (Fig. 5*M*). This effect, opposite to that observed in p57 overexpressing cells, supports a role for p57 in normal process outgrowth during development, as cells transition from precursor to differentiated neuron.

Effects of p57 and p27 Overexpression on Cell Cycle Exit, Neuronal/Glial Fate, and Differentiation of Cortical Progenitors In Vivo

To determine whether p57 may influence neurogenesis in the developing cerebral cortex, we introduced the same plasmid constructs used in culture into E15.5 rat brains by transuterine intracerebroventricular injections followed by electroporation, and studied effects on cell cycle exit and differentiation in cortical progenitors. One day after surgery, EGFP colocalized with high levels of p57 or p27 proteins detected by immunoreactivity in cortical VZ cells transfected with the respective plasmids, validating the efficacy of in vivo transfections (Supplementary Fig. S5*A–D*). Moreover, no activated caspase-3 signal was detected in electroporated cells 3 days after electroporation whatever the vector used, suggesting CKI overexpression had no effect on cell survival in vivo (data not shown).

We analyzed the effects of CKIs on cell cycle exit by counting the percent of EGFP+ cells entering S-phase in the VZ at 24 h. The proportion of BrdU-labeled cells was markedly decreased in CKI overexpressing cells, indicating that forced CKI expression elicited cell cycle arrest in vivo (Fig. 6*A–C*). In agreement with our in vitro results, Nterp57 blocked the cell cycle progression in vivo as well, while more VZ cells electroporated with Cterp57 incorporated BrdU than the control (Fig. 6*A*), supporting the hypothesis that the C-terminal part of p57 may play a role in cell proliferation control opposite to that of the N-terminal portion.

To analyze effects of CKIs on neuronal/glial differentiation in vivo, we examined colocalization of EGFP with related cell type markers. For neuronal differentiation, we assessed sections for βIII-tubulin immunolabeling. The labeling appeared increased in the VZ of the cortical area electroporated with p57 plasmid compared with a cortex electroporated with the control vector, a neighboring tissue devoid of green signal or the contralateral cortex (Fig. 6*D–K*).

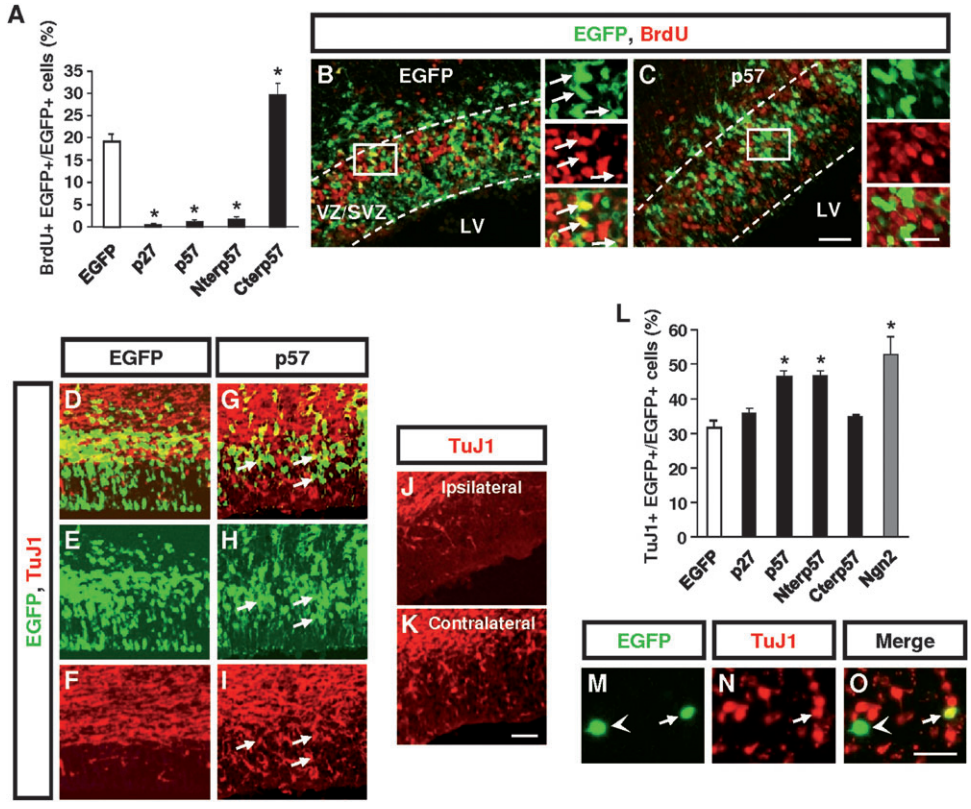

Figure 6. Effects of p57 and p27 overexpression on cell cycle exit and neuronal differentiation of cortical progenitors in vivo. One day after electroporation performed at E15.5, pregnant rats were injected subcutaneously with BrdU 2 h prior to sacrifice. After fixation and cryosectioning, tissues were processed for BrdU or TuJ1 immunostaining. (*A*) The fraction of EGFP+ VZ cells incorporating BrdU was reduced in p27, p57, and Nterp57 transfected cells. In contrast, more cells electroporated with Cterp57 plasmid were BrdU+. Data represent means ± SEM (n = 4–7 embryos/vector, 4 litters, 400–1000 EGFP+ cells, *$P < 0.01$). (*B*, *C*) Double labeling for EGFP (green) and BrdU (red) on sections of E16.5 brains electroporated at E15.5 with control EGFP (*B*) or p57 (*C*). Higher magnifications of insets show BrdU signal in cells transfected with control (arrows) and the absence of BrdU labeling in cells electroporated with p57. (*D–K*) TuJ1 immunostaining seems to be increased in the VZ of the cortical area exhibiting prominent p57 transfected cells (*G–I*) compared with the VZ of a cortex electroporated with control EGFP (*D–F*), a neighboring area without EGFP signal (*J*) and the contralateral part of the cortex (*K*). *D* and *G* are merged images of *E* and *F* and *H* and *I*, respectively. Arrows indicate double EGFP+ TuJ1+ cells. (*L–O*) To facilitate analysis, cortices were dissociated 1 day after electroporation (E16.5) and plated for 2 h prior to fixation and TuJ1 immunolabeling. Cells were counted in 12–15 random nonoverlapping fields. (*L*) More precursor cells electroporated with p57, Nterp57, and Ngn2 differentiated into TuJ1+ neurons compared with the control. No difference was obtained after electroporation with p27 or Cterp57. Data are means ± SEM (n = 3–5 embryos, 4 litters, 250–300 cells/vector, *$P < 0.01$). (*M–O*) Double labeling for EGFP (green) and TuJ1 (red) after electroporation with p57. Arrow indicates an EGFP+ cell labeled for TuJ1. Arrowhead identifies an EGFP+ TuJ1− cell. Scale bars: 50 μm (*B*, *C*, left panels; *D–K*), 25 μm (*B*, *C*, right panels; *M–O*).

However, counting of double-labeled cells on sections by confocal microscopy was hampered by the cytoplasmic localization of the βIII-tubulin immunoreactivity. To facilitate analysis, cells from cortices electroporated at E15.5 were dissociated at E16.5 and plated for 2 h before fixation and immunolabeling (Sanada and Tsai 2005). We found that p57 overexpression increased βIII-tubulin expressing cells by 48%, (Fig. 6*L–O*). In contrast, p27 overexpression had no effect at this time (Fig. 6*L*). However, by 48 h, p57 and p27 both increased the number of cells labeled for βIII-tubulin (EGFP: 55.1 ± 4.02%; p27: 77.6 ± 1.82%; p57: 78.3 ± 1.62%; n = 4–5 embryos; $P < 0.01$). These data parallel the in vitro βIII-tubulin results and indicate that p57 induces neuronal differentiation in vivo more precociously than p27 at this developmental stage. Moreover, the effect of p57 in vivo on βIII-tubulin was similar to that of Ngn2 (Fig. 6*L*). Finally, in agreement with the in vitro data, Nterp57 promoted neuronal differentiation in vivo with the same efficacy as full-length p57, whereas there was no change in βIII-tubulin expressing cells following Cterp57 electroporation (Fig. 6*L*).

To determine whether CKI overexpression affects astroglial differentiation in vivo, we electroporated embryos at E15.5 and assessed E18.5–19.5 brain sections for GFAP immunostaining. While GFAP+ fibers were revealed in the ventral telencephalon, no GFAP signal was detected in the cortex at these embryonic stages, regardless of which vector was injected (data not shown). We thus extended our analyses of neuronal/glial cell fate to P10, using NeuN and GFAP markers. While cells electroporated with the control vector at E15.5 did not exhibit any GFAP signal, some cells transfected with p57 and p27 expressed GFAP at P10 (Fig. 7*A*), the balance expressing NeuN. Furthermore, since our in vitro transfection data suggested that CKI effects on cell fate and differentiation may depend on developmental stage, we also performed in utero electroporation at E18.5 and analyzed electroporated cells at P10. Cells transfected with the control vector were strictly NeuN+ and accumulated in cortical layers II–III, consistent with the inside-out pattern of corticogenesis (Fig. 7*B,C,E-H*). While the majority of CKI transfected cells also settled in the upper layers and expressed NeuN, 10.5% and 13.8% of cells overexpressing p57 and p27, respectively, were GFAP+ and were scattered throughout the cortical wall (Fig. 7*B,D,I–P*). Together, these results indicate that p57 and p27 promote precocious neuronal and astrocyte differentiation. However, the amplitude of

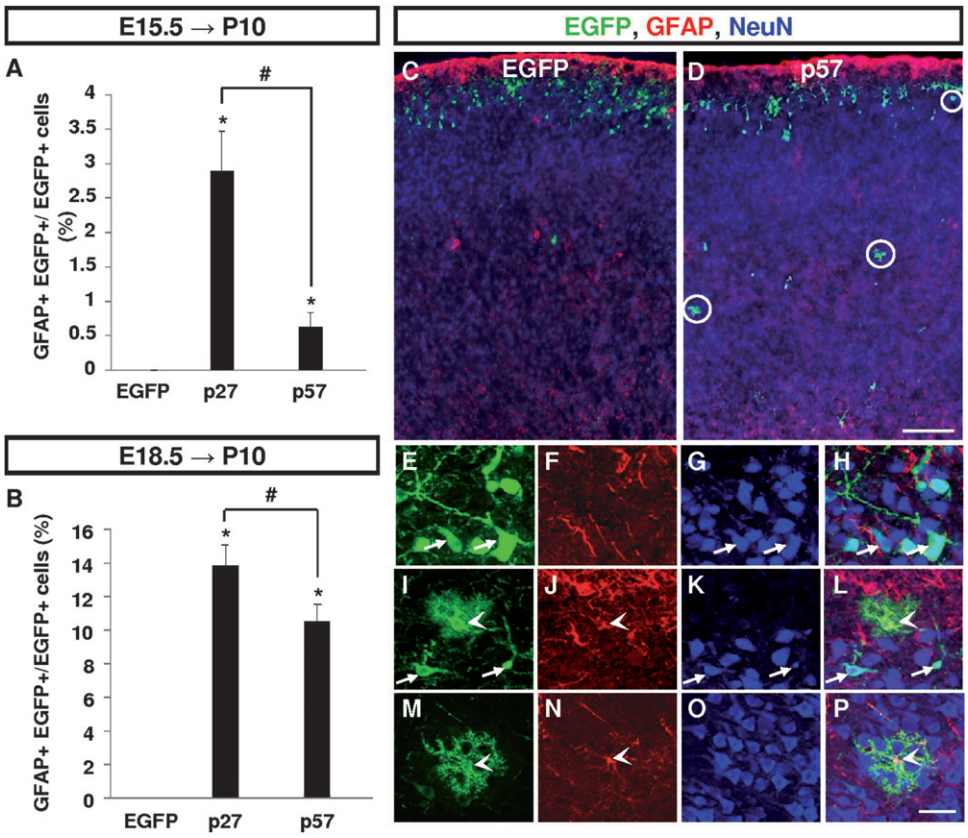

Figure 7. Effects of p57 and p27 overexpression on astroglial differentiation of cortical progenitors in vivo. Embryos electroporated at E15.5 or E18.5 were sacrificed and perfused at P10. After cryosectioning, brain tissues were processed for EGFP, GFAP, and NeuN triple immunostaining. (*A*, *B*) The proportion of cells expressing GFAP+ signal over the total number of electroporated cells was counted on 4 sections per animal. While cells transfected with the control vector at E15.5 (*A*) or E18.5 (*B*) did not exhibit any GFAP signal at P10, some p27 and p57 overexpressing cells expressed the astrocyte marker, with a greater proportion of GFAP+ cells following electroporation at E18.5 (*B*) compared with cells transfected at E15.5 (*A*). (*C*, *D*) Low magnification of triple immunostaining for EGFP (green), GFAP (red), and NeuN (blue) after electroporation at E18.5 with the empty (*C*) or p57 (*D*) vector. Neurons (labeled for NeuN) generated from precursors transfected at E18.5 with EGFP (*C*) or p57 (*D*) accumulated in upper cortical layers. In contrast, GFAP+ p57 electroporated cells were scattered throughout the cortical wall (*D*, circles). (*E–P*) Representative higher magnifications of triple immunolabeling of cells transfected with the control (*E–H*) or p57 plasmid (*I–P*). *H*, *L*, *P* are merged images of *E*, *F*, *G*, and *I*, *J*, *K*, and *M*, *N*, *O*, respectively. (*I–L*) p57-transfected cells labeled for GFAP or NeuN in the upper cortical layers. (*M–P*) GFAP+ p57 overexpressing cell in the deeper cortical layers (circled in *D*). Arrows show colocalization of EGFP and NeuN expression and arrowheads identify EGFP+ GFAP+ double-labeled cells. Data represent means ± SEM, n = 4–7 embryos/vector, 1000–3000 EGFP+ cells, $P < 0.001$ using the one-way analysis of variance followed by Dunnett post hoc test; $\#P < 0.05$, using unpaired Student's t test. Scale bars: 200 μm (*C*, *D*), 25 μm (*E–P*).

astrocyte induction differs between the 2 CKIs in favor of p27 (Fig. 7*A,B*) and depends on the developmental stage.

p57 and p27 Overexpression Promotes Cortical Cell Radial Migration

While previous studies suggested that p27 influences neuronal migration in developing mouse neocortex (Nguyen et al. 2006; Itoh et al. 2007), they were inconsistent regarding p57. Thus, we performed in utero electroporation in E15.5 rat embryos and analyzed the distribution of CKI transfected cells at both E18.5 and E19.5. In accordance with Nguyen et al. (2006), the number of migrating EGFP+ cells increased in the CP and decreased in the VZ/SVZ following p27 overexpression compared with control at E18.5 (Fig. 8*A,C,D*). While no change was observed at E18.5 following p57 electroporation (Fig. 8*A,C,E*), the number of cells accumulating in the upper part of the CP was increased at E19.5 (Fig. 8*B,F,G*). In comparison, Ngn2 overexpression markedly enhanced cortical migration at 4 days, as previously reported (Hand et al. 2005), with however a greater effect than p57 (Fig. 8*B,F,G,K*). These observations suggest that both p57 and p27 enhance cortical neuronal migration, though with different temporal profiles and potentially distinct mechanisms.

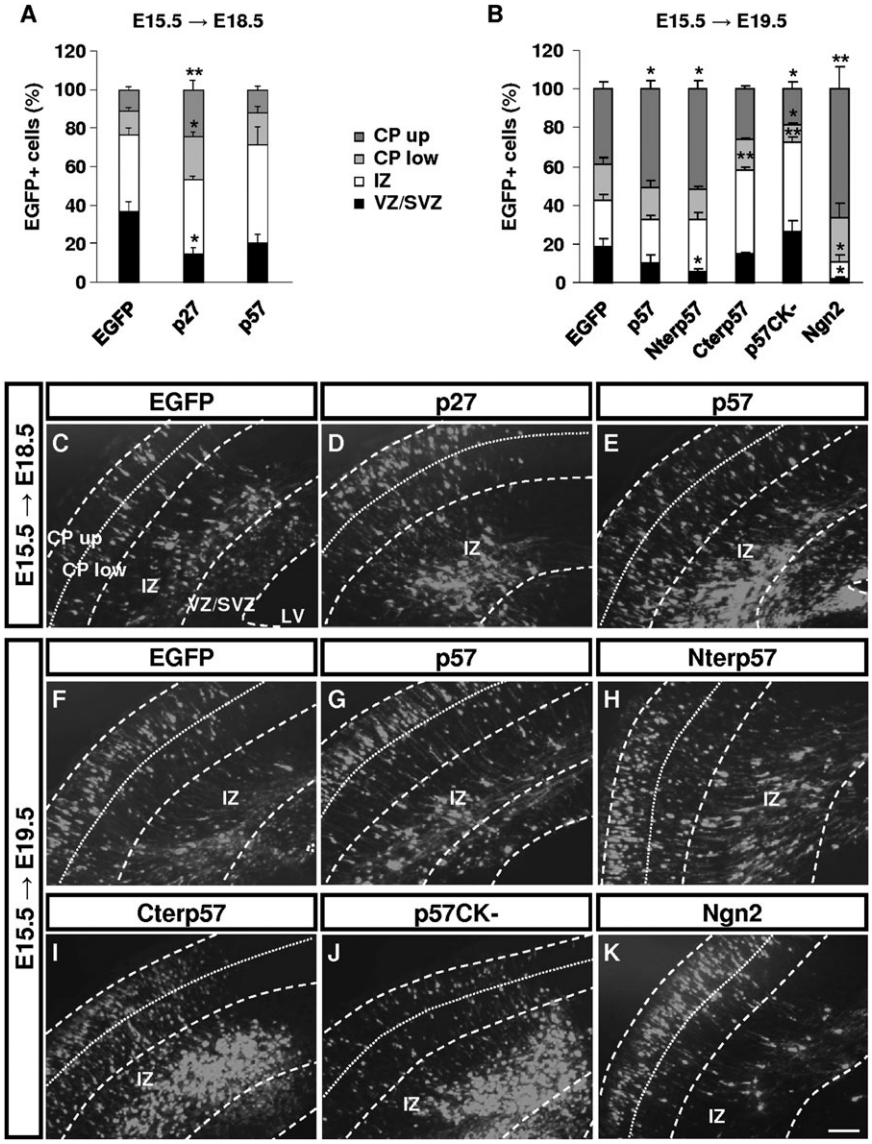

Figure 8. Effects of CKI overexpression on radial cell migration in developing rat cortex. The distribution of EGFP+ cells in the cortex was analyzed on coronal sections of E18.5 and E19.5 brains following electroporation at E15.5. The different cortical zones (VZ/SVZ, IZ, and CP) were delimited using propidium iodide staining (not shown). The CP was divided into 2 zones with equal height (CP low and CP up). (*A*) p27 overexpression significantly enhanced radial migration of cortical cells at 3 days (E18.5), as shown by the increase in number of cells reaching both CP zones. (*B*) p57 and Nterp57 overexpression significantly increased the number of cells reaching the upper part of the CP at 4 days (E19.5). By comparison, Ngn2 overexpression even more strongly enhanced radial migration. In contrast, a greater proportion of cells overexpressing Cterp57 and p57CK− remained in the IZ after 4 days. (*C–K*) Representative sections showing the position of EGFP+ cells in the different zones of the cortex, 3 days (*C–E*), or 4 days (*F–K*) after electroporation with control EGFP (*C*, *F*), p27 (*D*), p57 (*E*, *G*), Nterp57 (*H*), Cterp57 (*I*), p57CK− (*J*), or Ngn2 (*K*) plasmids. Data represent means ± SEM. Cells were counted in the dorsolateral region of the cortex on one section where a majority of transfected cells were identified plus one section 2 to 4 sections away. At 3 days, 4–6 animals/group were examined and at 4 days, 3–7 animals were assessed (total number of cells: control, Nterp57, Cterp57, p57CK− = 650–950 EGFP+ cells; p27, p57, Ngn2 = 150–300 EGFP+ cells; $*P < 0.05$, $**P < 0.01$). Scale bar: 100 μm (*C–K*). CP low, lower part of the CP; CP up, upper part of the CP.

We considered the possibility that differences in migration effects might be attributable to differences in protein levels. Thus, we compared the distance that electroporated cells migrated as a function of intensity of p27 and p57 immunofluorescence. We found no correlation between immunofluorescence intensity and distance of migration (Supplementary Fig. S5*E,F*), indicating that effects on cell migration do not depend on the quantity of overexpressed protein. Moreover, the 2 CKIs did not appear to alter the radial glial scaffolding based on the morphology of nestin immunolabeled fibers (data not shown), suggesting a cell autonomous effect on cell migration.

We extended our analyses on migration and positioning of p57 electroporated cells to after birth, when cortical cell migration is completed. Cortices of P10 brains electroporated at E15.5 were divided into 9 equal bins. In agreement with the prenatal observations, we found that more p57 transfected cells accumulated in the upper bins (1–4) than the control, while no difference was detected in the lower bins (5–9) (Fig. 9*A–F*). Since bins 1–4 roughly corresponded to cortical layers II–IV, we analyzed cell migration/position in the upper layers II–III defined with specific marker Cux1. While no change was measured in the total proportion of cells settled in the Cux1 layer (EGFP: 40.5 ± 5.59%; p57: 41.9 ± 8.40%, $P > 0.05$), a larger proportion of p57-transfected cells were located in the upper half of the layer (Fig. 9*G–K*). These results suggest that p57 does not likely alter laminar phenotype but rather influences cell positioning within the layer of destination.

Finally, we analyzed the effects of Nterp57 and Cterp57 overexpression on neuronal migration in vivo. Contrary to the N-terminal part of p27 (Nguyen et al. 2006), Nterp57 overexpression promoted cell migration as effectively as the full-length protein (Fig. 8*B,G,H*). In contrast, Cterp57 overexpressing cells accumulated in the IZ 4 days after electroporation

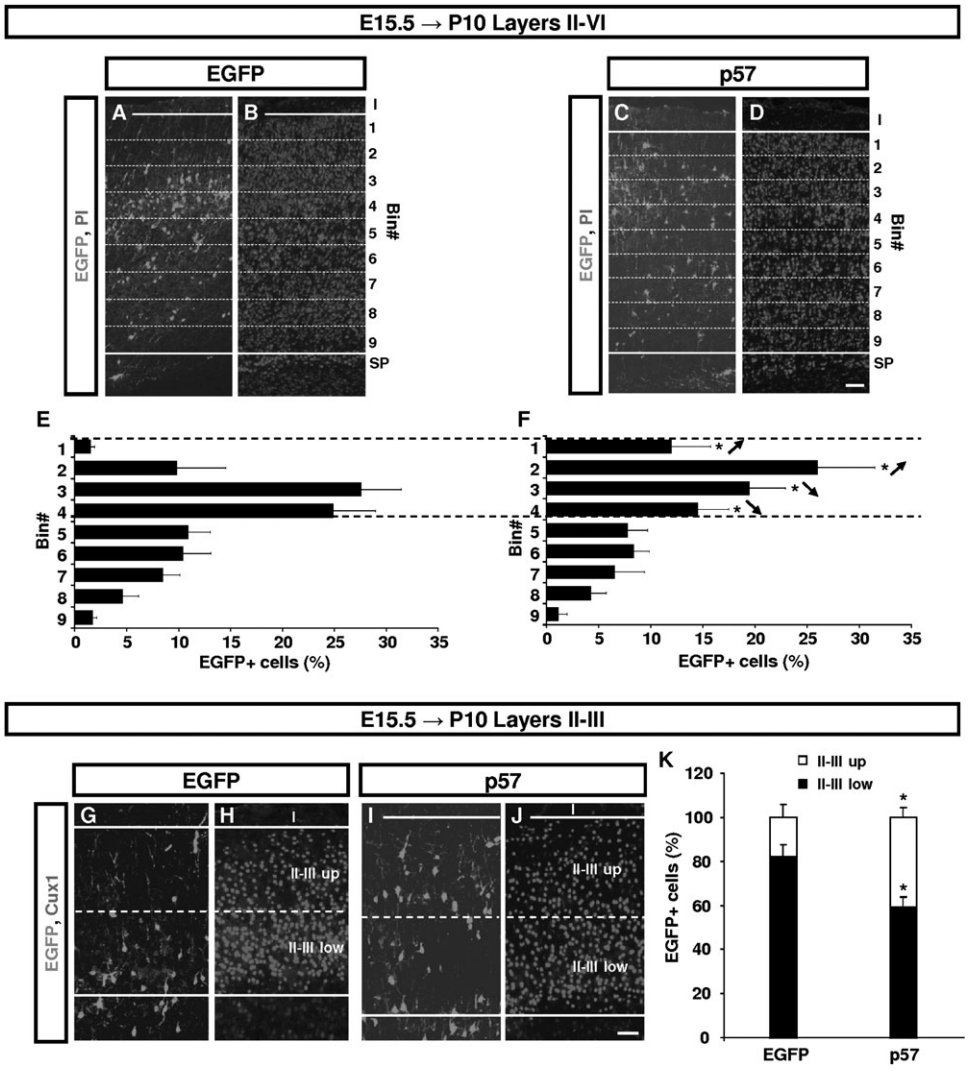

Figure 9. Effects of p57 overexpression on radial migration and cell positioning in postnatal cortex. (*A–F*) The distribution of cells electroporated at E15.5 with control EGFP (*A*, *B*) or p57 (*C*, *D*) plasmids was analyzed on coronal sections of P10 brains stained with propidium iodide (PI). The radial extent of the cortical wall was divided into 9 bins of equivalent height from layers VI to II (*A*, *D*). The proportion of p57 overexpressing cells settled in the upper bins was higher (*F*) than the control (*E*). (*G–K*) The distribution of cells transfected with EGFP (*G–H*) or p57 (*I*, *J*) was analyzed within the superficial layers II–III (labeled for Cux1, red). Layers II–III were divided into 2 zones of equivalent height (II–III low and II–III up). More p57 electroporated cells migrated in the upper half of the layers II–III (*K*). I, Layer I; II-III low, lower part of layers II-III; II-III up, upper part of layers II-III; SP, subplate. Data represent means ± SEM ($n = 5–7$ pups, 500–700 EGFP+ cells, $^*P < 0.05$, compared with the corresponding bin in the control, using Student's *t* test). Scale bars: 100 μm (*A–D*), 50 μm (*G–J*).

(Fig. 8*B,F,I*). To determine whether these cells in the IZ were actively dividing precursors or postmitotic neurons, we performed double immunolabeling with neural progenitor markers Pax6 and Tbr2 and neuronal marker βIII-tubulin. Virtually no electroporated cells expressed either Pax6 or Tbr2 (data not shown) but they were positive for neuronal marker βIII-tubulin (Supplementary Fig. S6*A–F*). In addition, we did not detect any electroporated cells labeled for astrocyte marker GFAP or oligodendrocyte marker CC1 (data not shown). These observations suggest that Cterp57 overexpression may impair neuronal radial migration. However, since Cterp57 overexpression stimulated proliferation 24 h after electroporation in vivo, we cannot exclude that accumulation of neurons in the IZ 4 days after electroporation may be caused by the increased number of progenitors in the VZ/SVZ days before.

p57 Effects on Cell Differentiation and Migration Depend on the Cyclin/CDK Binding/Inhibitory Sites

CKIs clearly exhibit additional functions that are not linked to cell cycle control (Ohnuma et al. 1999; Joseph et al. 2003; Nguyen et al. 2006). To determine whether effects of p57 are related to cell cycle exit, we generated a p57 mutant vector (p57CK-) deficient for interaction with both cyclins and CDKs.

In vitro transfection of E14.5 cortical cells with p57CK– lead to high levels of p57 protein at 24 h (Supplementary Fig. S7*A–C*). Contrary to the WT form, the cell cycle mutant of p57 did not promote cell cycle exit, with a BrdU-labeling index at 48 h similar to that of the control (Supplementary Fig. S7*D–G*). The mutant form did not induce neuronal differentiation in culture since no difference in the proportion of βIII-tubulin+ cells was observed in comparison with the control at 48 h (Supplementary Fig. S7*H*). Likewise, p57CK– did not induce astrocyte differentiation of E17.5 precursors in vitro with a percentage of GFAP+ cells similar to the control (Supplementary Fig. S7*I*). p57CK– expression also did not affect process outgrowth with an average length of the longest process close to that of the control at 48 h (Supplementary Fig. S7*J*).

In vivo, cells electroporated with p57CK– mutant expressed high levels of p57 protein (Supplementary Fig. S7*K*) and incorporated BrdU normally (Supplementary Fig. S7*L,M*). βIII-tubulin immunostaining of cells dissociated from cortices 24 h after electroporation indicated that p57CK– did not significantly alter neuronal differentiation in vivo (Supplementary Fig. S7*N*). Furthermore, p57CK– transfection did not promote cortical cell migration. On the contrary and similar to Cterp57, more p57CK– transfected cells accumulated in the IZ 4 days after electroporation while less reached the CP (Fig. 8*B,F,I, J*). Double immunolabeling with βIII-tubulin indicated that cells accumulating in the IZ were postmitotic neurons (not shown), suggesting that p57CK– impaired neuronal migration independently of a role on precursor proliferation. Altogether, these experiments suggest that p57 effects on cortical neuronal differentiation and migration require cyclin/CDK binding/inhibitory domains.

Discussion

Our observations indicate that p57 and p27 have similar as well as differential effects during corticogenesis. While they both induce cell cycle exit, differentiation, neurite outgrowth, and migration, the amplitude of their effects is not equivalent. Interestingly, they differentially regulate neuronal/glial cell fate depending on environmental signals. Moreover, the analogous molecular domains of the CKIs exert both common as well as distinct functions. Contrary to p27, all developmental effects of p57 require the cyclin/CDK binding/inhibitory domains, suggesting the 2 CKIs regulate corticogenesis through different molecular pathways.

CKI Expression and Regulation in Cortical Precursors

Cip/Kip genes exhibited distinct temporal expression profiles during embryonic cortical development. While p57 mRNA was more abundant at early/middle stages, p27 was highly expressed at late stages, suggesting that they play similar or distinct roles at different stages of corticogenesis. p57 and p27 proteins were mainly expressed in postmitotic compartments in cerebral cortex, with fewer cells in the proliferative zone, suggesting roles in several stages of corticogenesis. Interestingly, p57 was expressed in groups of cycling precursors and postmitotic cells in the VZ/SVZ, suggesting a role in the transition from precursor proliferation to differentiation. These observations diverge with previous reports showing p57 protein localized to the CP with faint expression in the IZ and no signal in the VZ/SVZ (Nguyen et al. 2006; Itoh et al. 2007). This discrepancy is likely due to the different antibodies and/or fixation methods used for p57 detection. The immunolabeling we observed is specific to p57 since 1) no signal was detected in p57KO brains by immunohistochemistry and 2) is consistent with p57 expression detected by in situ hybridization in VZ/SVZ and CP in embryonic rat cortex (van Lookeren Campagne and Gill 1998).

p57 and p27 mRNA levels were decreased by mitogenic bFGF, consistent with previous studies and their role in cell cycle exit (Frederick and Wood 2004; Li and DiCicco-Bloom 2004). As described previously (Itoh et al. 2007), p57 and p27 mRNA levels, as Ngn2, were increased upon neuronal differentiation induced by mitogen withdrawal, supporting a role for CKIs in neurogenesis. However, only p57 and Ngn2 expression was increased in E14.5 precursors following antimitogenic PACAP exposure, supporting that PACAP selectively regulates p57 expression (Carey et al. 2002). In contrast, no difference in p57 expression was detected after PACAP treatment of E17.5 cells, suggesting that effects are mediated through different mechanisms depending on developmental stage. While NT-3 increased p57 levels in E14.5 precursors, it decreased p57, p27, and Ngn2 expression and increased DNA synthesis at E17.5, suggesting that NT-3 has opposite effects on proliferation/differentiation during early- and late-corticogenesis. Overall, these results suggest that p57 and p27 expression are differentially regulated and depend on both extracellular environment and developmental stage.

p57 and p27 Differentially Regulate Neuronal and Glial Differentiation in a Context-Dependent Manner

Our studies add further evidence that CKIs regulate cell fate and differentiation (Dyer and Cepko 2000; Ohnuma et al. 2001). Forced expression of p57 or p27 elicited robust cell cycle exit in vivo and in vitro. Cip/Kip proteins share a highly conserved cyclin/CDK binding/inhibitory domain in their N-terminal region that can block/delay cycle progression of progenitors from diverse tissues (Cunningham and Roussel 2001). In addition, both p57 and p27 overexpression induced premature precursor differentiation in vitro and in vivo, reducing expression of nestin and increasing Tbr1

and βIII-tubulin without altering cell death/survival. In agreement, in p57-deficient cortical cells, the precursor population expanded at the expense of differentiated cells. It remains to be determined whether p57 1) controls proliferation and differentiation independently, 2) acts solely on proliferation with effects on differentiation being a natural consequence, or 3) alters activity of some upstream master regulator of the transition from proliferation to differentiation. Our observations indicate that p57 promotes greater neuronal differentiation than p27 both in vitro and in vivo regardless of environmental signals or developmental stage, suggesting that p57 may serve as one factor biasing cells toward a neuronal fate. In the presence of CNTF, p57 enhanced neuronal differentiation but did not permit astrocyte differentiation of E14.5 precursors. In contrast, p27 increased both neuronal and glial differentiation, supporting a role for p27 in astrocyte differentiation as reported previously (Tikoo et al. 1997). At a late embryonic stage, when endogenous gliogenesis begins (Miller and Gauthier 2007; Faigle et al. 2008), both CKIs promoted gliogenesis in vitro and in vivo. However, p57 produced proportionally more neurons than astrocytes in vitro while p27 had the opposite effect. And in vivo, p57 produced 4-fold less astrocytes than p27 (E15.5–P10). Finally, p57 was not permissive to CNTF gliogenic effect contrary to the control and p27. These results suggest that CKIs may differently regulate cell fate/differentiation as a function of local environmental signals, as proposed previously (Ohnuma et al. 1999; Mochizuki et al. 2009). One may speculate that CKIs influence cell differentiation through differential interactions with lineage-specific transcription factors, though other models are possible. In contrast, Ngn2 instructs a neuronal fate by promoting neurogenesis and inhibiting gliogenesis regardless of extracellular environment, in agreement with previous studies (Sun et al. 2001).

p57 Regulates Process Outgrowth and Radial Migration

In vitro, p57-deficient cells grew shorter processes, while p57 overexpression enhanced process outgrowth, in both differentiated cells and precursors. These results suggest that p57 may play a role in the early stages of neuritogenesis including initiation of neurite formation and elongation (Tojima and Ito 2004) before precursors acquire a phenotype of differentiated neuron. However, p57 may also contribute to further stages, such as axon polarization and/or elongation (da Silva and Dotti 2002). In addition, p57-overexpressing cells extended longer processes than p27-transfected cells, suggesting that CKIs differentially regulate process outgrowth, potentially through distinct cytoskeleton pathways or affecting distinct progenitor populations. p57 can regulate actin dynamics by binding and translocating into the nucleus the serine/threonine kinase LIMK-1, a downstream regulator of Rho family GTPases that stabilize actin filaments (Yokoo et al. 2003; Heinen et al. 2008). Several studies suggest a role for CKIs and p27 in particular, in cell motility and migration through regulation of actin organization (Tanaka et al. 2002; Besson et al. 2004; Kawauchi et al. 2006; Nguyen et al. 2006).

In vivo, both p57 and p27 overexpression promoted cortical cell migration but at different times, p27 affecting migration before p57. p27 knock down in developing mouse neocortex impaired neuronal migration in both the IZ and CP (Kawauchi et al. 2006; Nguyen et al. 2006) while p57 RNA interference resulted in a significant delay in the CP only (Itoh et al. 2007). These observations suggest that functions of p57 and p27 in cell migration may not be redundant. The 2 CKIs may affect migration of distinct cell populations and/or different steps of radial migration, with p27 regulating migration from the VZ to CP, and p57 controlling proper positioning of neurons within the CP. Supporting this hypothesis, we found that intralaminar position of p57 overexpressing cells was altered in layers II–III in P10 cortices electroporated at E15.5, with more cells occupying the upper region compared with control cells.

Although unlikely, one might consider an alternative model in which p57 acts only on cell cycle exit, with changes in migration and differentiation as mere consequences. However, such precocious cell cycle exit induced by p57 overexpression would produce a cohort of cells with a slightly earlier birthdate, which cells in turn should localize to deeper layer II/III positions. In contrast, we found cells migrating past the usual laminar position to more superficial layers. These observations suggest that p57 also serves to independently regulate cell positioning. Further studies on migration mechanisms remain to be performed.

The N-terminal and C-terminal Regions of p57 Exhibit Opposite Functional Effects

Similar and distinct phenotypes were observed after overexpressing analogous molecular regions of p57 and p27. Consistent with their structural similarity, N-terminal regions of both CKIs can induce both cell cycle exit and differentiation (Nguyen et al. 2006). However, contrary to Nterp27 (Nguyen et al. 2006), Nterp57 also promoted migration. Furthermore, while the C-terminal region of p27 promoted cortical migration and minimally enhanced differentiation (Nguyen et al. 2006), Cterp57 stimulated proliferation and impaired neuronal migration, supporting the proposal that CKIs play distinct roles through their divergent C-terminal structures. In addition to the QT domain common to p57 and p27, Cterp57 contains unique proline rich and acidic domains (Nakayama 1998), which are involved in protein–protein interactions. Proline-rich domains are potential binding sites for Src homology 3 domains that are associated with various functions including signal transduction, cell polarization, and membrane–cytoskeleton interactions (Mayer 2001).

While our observations suggest that Nterp57 is necessary and sufficient to induce cell cycle exit, differentiation and migration, Cterp57 overexpression enhanced cell cycle progression in vitro and in vivo. While splice variants of p57 mRNA that generate proteins with different amino-terminal sequences have been detected in the rat (Potikha et al. 2005), to our knowledge, no isoforms with divergent C-terminal extremities have been reported. Intriguingly, the proliferative activity of Cterp57 is reminiscent of a previous study showing that the N- and C-terminal portions of human p27 play opposite regulatory roles in G2/M progression in Xenopus oocytes (Font de Mora et al. 1997). While the N-terminal portion is inhibitory, the C-terminal fragment activated $p34^{cdc2}$ kinase (CDK1) through direct interaction, likely increasing proliferation.

p57 Activities Require the Cyclin/CDK Binding/Inhibitory Domains

The mutant form of p57 lacking the cyclin/CDK binding/inhibitory domains, as expected, did not block cell cycle progression, but it also did not promote differentiation while it impaired neuronal migration, effects which contrast with the corresponding p27 mutant (Nguyen et al. 2006). These results

suggest that functions of p27 and p57 in cell differentiation and migration involve different pathways. While p27 activities are cell cycle independent (Nguyen et al. 2006), p57 effects apparently rely on cyclin/CDK binding/inhibitory domains. Since both CDK inhibitory activity and cyclin/CDK binding were suppressed by the mutations, 2 hypotheses should be considered: 1) p57 functions may require inhibition of CDK activity (cell cycle-dependent functions) or 2) they may only involve interactions with cyclin/CDK complexes but not the CDK inhibitory activity (cell cycle-independent functions). Consistent with the latter hypothesis, the role of p21 in Müller glial cell fate was shown to be independent of growth arrest but dependent on its interaction with cyclin D1/CDK4 complexes (Ohnuma et al. 1999).

In conclusion, p57 regulates multiple stages of corticogenesis, similar to p27. Since both CKIs promote the transition of neural precursors to all lineages of neural cells including neurons, astrocytes (our results), and oligodendrocytes (Casaccia-Bonnefil et al. 1997; Durand et al. 1997; Dugas et al. 2007), they do not likely act as determinant factors. Rather, they trigger differential cell responses to other intrinsic and extrinsic signals that may instruct a particular cell fate. Further investigations will need to define the common and/or distinct signaling pathways through which p57 and p27 differentially influence cell fate determination.

Supplementary Material

Supplementary material can be found at: http://www.cercor.oxfordjournals.org/

Funding

National Institutes of Health (R01 NS32401).

Notes

We thank Dr Pumin Zhang for providing p57 knockout mice, Dr Akiva Marcus for technical advice on in utero injections, Dr Paul Matteson for advice on plasmid constructions, and Xiaofeng Zhou, Elise Pasoreck, and Jaine-Iscia Gernet for technical support. *Conflict of Interest*: None declared.

References

Angevine JB Jr, Sidman RL. 1961. Autoradiographic study of cell migration during histogenesis of cerebral cortex in the mouse. Nature. 192:766–768.

Besson A, Dowdy SF, Roberts JM. 2008. CDK inhibitors: cell cycle regulators and beyond. Dev Cell. 14:159–169.

Besson A, Gurian-West M, Schmidt A, Hall A, Roberts JM. 2004. p27Kip1 modulates cell migration through the regulation of RhoA activation. Genes Dev. 18:862–876.

Bonni A, Sun Y, Nadal-Vicens M, Bhatt A, Frank DA, Rozovsky I, Stahl N, Yancopoulos GD, Greenberg ME. 1997. Regulation of gliogenesis in the central nervous system by the JAK-STAT signaling pathway. Science. 278:477–483.

Carey RG, Li B, DiCicco-Bloom E. 2002. Pituitary adenylate cyclase activating polypeptide anti-mitogenic signaling in cerebral cortical progenitors is regulated by p57Kip2-dependent CDK2 activity. J Neurosci. 22:1583–1591.

Casaccia-Bonnefil P, Tikoo R, Kiyokawa H, Friedrich V Jr, Chao MV, Koff A. 1997. Oligodendrocyte precursor differentiation is perturbed in the absence of the cyclin-dependent kinase inhibitor p27Kip1. Genes Dev. 11:2335–2346.

Cunningham JJ, Roussel MF. 2001. Cyclin-dependent kinase inhibitors in the development of the central nervous system. Cell Growth Differ. 12:387–396.

da Silva JS, Dotti CG. 2002. Breaking the neuronal sphere: regulation of the actin cytoskeleton in neuritogenesis. Nat Rev Neurosci. 3:694–704.

Dugas JC, Ibrahim A, Barres BA. 2007. A crucial role for p57(Kip2) in the intracellular timer that controls oligodendrocyte differentiation. J Neurosci. 27:6185–6196.

Durand B, Gao FB, Raff M. 1997. Accumulation of the cyclin-dependent kinase inhibitor p27/Kip1 and the timing of oligodendrocyte differentiation. EMBO J. 16:306–317.

Dyer MA, Cepko CL. 2000. p57(Kip2) regulates progenitor cell proliferation and amacrine interneuron development in the mouse retina. Development. 127:3593–3605.

Dyer MA, Cepko CL. 2001. The p57Kip2 cyclin kinase inhibitor is expressed by a restricted set of amacrine cells in the rodent retina. J Comp Neurol. 429:601–614.

Faigle R, Liu L, Cundiff P, Funa K, Xia Z. 2008. Opposing effects of retinoid signaling on astrogliogenesis in embryonic day 13 and 17 cortical progenitor cells. J Neurochem. 106:1681–1698.

Fero ML, Rivkin M, Tasch M, Porter P, Carow CE, Firpo E, Polyak K, Tsai LH, Broudy V, Perlmutter RM, et al. 1996. A syndrome of multiorgan hyperplasia with features of gigantism, tumorigenesis, and female sterility in p27(Kip1)-deficient mice. Cell. 85:733–744.

Font de Mora J, Uren A, Heidaran M, Santos E. 1997. Biological activity of p27kip1 and its amino- and carboxy-terminal domains in G2/M transition of Xenopus oocytes. Oncogene. 15:2541–2551.

Frederick TJ, Wood TL. 2004. IGF-I and FGF-2 coordinately enhance cyclin D1 and cyclin E-cdk2 association and activity to promote G1 progression in oligodendrocyte progenitor cells. Mol Cell Neurosci. 25:480–492.

Ge W, He F, Kim KJ, Blanchi B, Coskun V, Nguyen L, Wu X, Zhao J, Heng JI, Martinowich K, et al. 2006. Coupling of cell migration with neurogenesis by proneural bHLH factors. Proc Natl Acad Sci U S A. 103:1319–1324.

Hand R, Bortone D, Mattar P, Nguyen L, Heng JI, Guerrier S, Boutt E, Peters E, Barnes AP, Parras C, et al. 2005. Phosphorylation of Neurogenin2 specifies the migration properties and the dendritic morphology of pyramidal neurons in the neocortex. Neuron. 48:45–62.

Heinen A, Kremer D, Hartung HP, Kury P. 2008. p57 kip2's role beyond Schwann cell cycle control. Cell Cycle. 7:2781–2786.

Itoh Y, Masuyama N, Nakayama K, Nakayama KI, Gotoh Y. 2007. The cyclin-dependent kinase inhibitors p57 and p27 regulate neuronal migration in the developing mouse neocortex. J Biol Chem. 282:390–396.

Joseph B, Wallen-Mackenzie A, Benoit G, Murata T, Joodmardi E, Okret S, Perlmann T. 2003. p57(Kip2) cooperates with Nurr1 in developing dopamine cells. Proc Natl Acad Sci U S A. 100:15619–15624.

Kawauchi T, Chihama K, Nabeshima Y, Hoshino M. 2006. Cdk5 phosphorylates and stabilizes p27kip1 contributing to actin organization and cortical neuronal migration. Nat Cell Biol. 8:17–26.

Koguchi K, Nakatsuji Y, Nakayama K, Sakoda S. 2002. Modulation of astrocyte proliferation by cyclin-dependent kinase inhibitor p27(Kip1). Glia. 37:93–104.

Li B, DiCicco-Bloom E. 2004. Basic fibroblast growth factor exhibits dual and rapid regulation of cyclin D1 and p27 to stimulate proliferation of rat cerebral cortical precursors. Dev Neurosci. 26:197–207.

Lu N, DiCicco-Bloom E. 1997. Pituitary adenylate cyclase-activating polypeptide is an autocrine inhibitor of mitosis in cultured cortical precursor cells. Proc Natl Acad Sci U S A. 94:3357–3362.

Mairet-Coello G, Tury A, DiCicco-Bloom E. 2009. Insulin-like growth factor-1 promotes G(1)/S cell cycle progression through bidirectional regulation of cyclins and cyclin-dependent kinase inhibitors via the phosphatidylinositol 3-kinase/Akt pathway in developing rat cerebral cortex. J Neurosci. 29:775–788.

Mayer BJ. 2001. SH3 domains: complexity in moderation. J Cell Sci. 114:1253–1263.

McConnell SK, Kaznowski CE. 1991. Cell cycle dependence of laminar determination in developing neocortex. Science. 254:282–285.

Megason SG, McMahon AP. 2002. A mitogen gradient of dorsal midline Wnts organizes growth in the CNS. Development. 129:2087–2098.

Miller FD, Gauthier AS. 2007. Timing is everything: making neurons versus glia in the developing cortex. Neuron. 54:357–369.
Mochizuki T, Bilitou A, Waters CT, Hussain K, Zollo M, Ohnuma S. 2009. Xenopus NM23-X4 regulates retinal gliogenesis through interaction with p27Xic1. Neural Dev. 4:1.
Nakayama K. 1998. Cip/Kip cyclin-dependent kinase inhibitors: brakes of the cell cycle engine during development. Bioessays. 20:1020–1029.
Nakayama K, Ishida N, Shirane M, Inomata A, Inoue T, Shishido N, Horii I, Loh DY. 1996. Mice lacking p27(Kip1) display increased body size, multiple organ hyperplasia, retinal dysplasia, and pituitary tumors. Cell. 85:707–720.
Nguyen L, Besson A, Heng JI, Schuurmans C, Teboul L, Parras C, Philpott A, Roberts JM, Guillemot F. 2006. p27kip1 independently promotes neuronal differentiation and migration in the cerebral cortex. Genes Dev. 20:1511–1524.
Ohnuma S, Philpott A, Harris WA. 2001. Cell cycle and cell fate in the nervous system. Curr Opin Neurobiol. 11:66–73.
Ohnuma S, Philpott A, Wang K, Holt CE, Harris WA. 1999. p27Xic1, a Cdk inhibitor, promotes the determination of glial cells in Xenopus retina. Cell. 99:499–510.
Perez-Martinez L, Jaworski DM. 2005. Tissue inhibitor of metalloproteinase-2 promotes neuronal differentiation by acting as an anti-mitogenic signal. J Neurosci. 25:4917–4929.
Potikha T, Kassem S, Haber EP, Ariel I, Glaser B. 2005. p57Kip2 (cdkn1c): sequence, splice variants and unique temporal and spatial expression pattern in the rat pancreas. Lab Invest. 85:364–375.
Rakic P. 1974. Neurons in rhesus monkey visual cortex: systematic relation between time of origin and eventual disposition. Science. 183:425–427.
Sanada K, Tsai LH. 2005. G protein betagamma subunits and AGS3 control spindle orientation and asymmetric cell fate of cerebral cortical progenitors. Cell. 122:119–131.
Sherr CJ, Roberts JM. 1999. CDK inhibitors: positive and negative regulators of G1-phase progression. Genes Dev. 13:1501–1512.
Song JH, Wang CX, Song DK, Wang P, Shuaib A, Hao C. 2005. Interferon gamma induces neurite outgrowth by up-regulation of p35 neuron-specific cyclin-dependent kinase 5 activator via activation of ERK1/2 pathway. J Biol Chem. 280:12896–12901.
Song MR, Ghosh A. 2004. FGF2-induced chromatin remodeling regulates CNTF-mediated gene expression and astrocyte differentiation. Nat Neurosci. 7:229–235.
Sun Y, Nadal-Vicens M, Misono S, Lin MZ, Zubiaga A, Hua X, Fan G, Greenberg ME. 2001. Neurogenin promotes neurogenesis and inhibits glial differentiation by independent mechanisms. Cell. 104:365–376.
Tanaka H, Yamashita T, Asada M, Mizutani S, Yoshikawa H, Tohyama M. 2002. Cytoplasmic p21(Cip1/WAF1) regulates neurite remodeling by inhibiting Rho-kinase activity. J Cell Biol. 158:321–329.
Tikoo R, Casaccia-Bonnefil P, Chao MV, Koff A. 1997. Changes in cyclin-dependent kinase 2 and p27kip1 accompany glial cell differentiation of central glia-4 cells. J Biol Chem. 272:442–447.
Tojima T, Ito E. 2004. Signal transduction cascades underlying de novo protein synthesis required for neuronal morphogenesis in differentiating neurons. Prog Neurobiol. 72:183–193.
van Lookeren Campagne M, Gill R. 1998. Tumor-suppressor p53 is expressed in proliferating and newly formed neurons of the embryonic and postnatal rat brain: comparison with expression of the cell cycle regulators p21Waf1/Cip1, p27Kip1, p57Kip2, p16Ink4a, cyclin G1, and the proto-oncogene Bax. J Comp Neurol. 397:181–198.
Watanabe H, Pan ZQ, Schreiber-Agus N, DePinho RA, Hurwitz J, Xiong Y. 1998. Suppression of cell transformation by the cyclin-dependent kinase inhibitor p57KIP2 requires binding to proliferating cell nuclear antigen. Proc Natl Acad Sci U S A. 95:1392–1397.
Ye W, Mairet-Coello G, DiCicco-Bloom E. 2007. DNAse I pre-treatment markedly enhances detection of nuclear cyclin-dependent kinase inhibitor p57Kip2 and BrdU double immunostaining in embryonic rat brain. Histochem Cell Biol. 127:195–203.
Yokoo T, Toyoshima H, Miura M, Wang Y, Iida KT, Suzuki H, Sone H, Shimano H, Gotoda T, Nishimori S, et al. 2003. p57Kip2 regulates actin dynamics by binding and translocating LIM-kinase 1 to the nucleus. J Biol Chem. 278:52919–52923.
Zezula J, Casaccia-Bonnefil P, Ezhevsky SA, Osterhout DJ, Levine JM, Dowdy SF, Chao MV, Koff A. 2001. p21cip1 is required for the differentiation of oligodendrocytes independently of cell cycle withdrawal. EMBO Rep. 2:27–34.
Zhang P, Liegeois NJ, Wong C, Finegold M, Hou H, Thompson JC, Silverman A, Harper JW, DePinho RA, Elledge SJ. 1997. Altered cell differentiation and proliferation in mice lacking p57KIP2 indicates a role in Beckwith-Wiedemann syndrome. Nature. 387:151–158.